Introduction

Phagocytic cells like monocytes, macrophages, neutrophils and eosinophils, play an essential role in innate host defence against infectious agents by oxidative and nonoxidative antimicrobial mechanisms. Once an inflammatory response is initiated, circulating neutrophils are recruited by chemoattractants, released from bacteria or endogenously generated by the host (e.g. N-formyl peptides, bacterial LPS, complementary factor C5α and leukotriene B4), in the inflammatory sites. Neutrophils recognize opsonized pathogens (e.g. iC3b, Ab) via their membrane receptors (e.g. CD3, CD4, FcRγII) and engulf them by the process known as phagocytosis (Figure 1), which was observed for the first time by Metchnikoff in 1883. An enhanced 'respiration' of leukocytes during phagocytosis was observed in 1933 by Balbridge and Gerard (Balbridge et al. 1933). In 1959 Sbarra and Karnovsky discovered that this specific increase in oxygen consumption was resistant to conventional inhibitors of mitochondrial respiration (Sbarra et al. 1959). This 'respiratory burst' was soon discovered to be a requirement for the efficient bacterial killing by neutrophils (Selvaraj et al. 1966). Failure in 'respiratory burst' during phagocytosis resulted in a syndrome, the 'fatal granulomatosis of childhood' (Holmes et al. 1967), now referred as chronic granulomatous disease (CGD). Glycolysis demonstrated to provide the necessary energy for phagocytosis and degranulation. The increase in oxidation of glucose via hexose monophosphate shunt coincident during the activation of the respiratory burst, suggested that NADPH was the most likely candidate (Rossi et al. 1964). As a result, this enzyme system had become known as the NADPH oxidase.

1. Bacterial killing mechanism

1.1 Reactive oxygen species production (ROS)

Upon activation, the NADPH oxidase catalyses the formation of superoxide from oxygen and NADPH, according to the following reaction:

$$NADPH + 2O_2 \xrightarrow{\text{NADPH oxidase}} NADP^+ + H^+ + 2O_2^{-\bullet}$$

The superoxide anion is both a one-electron reductant and a one-electron oxidant that can pass through the cell membrane. It appears that superoxide anions do not have direct toxic effects on bacteria or fungi. But they can be converted to other reactive oxygen species (ROS). Most superoxide spontaneously or catalytically by superoxide dismutase (SOD) dismutates to H_2O_2 and O_2:

$$O_2^{-\bullet} + O_2^{-\bullet} + 2H^+ \xrightarrow{\text{SOD}} O_2 + H_2O_2$$

H_2O_2 is not very toxic, it interacts with myeloperoxidase (MPO), contained in neutrophil

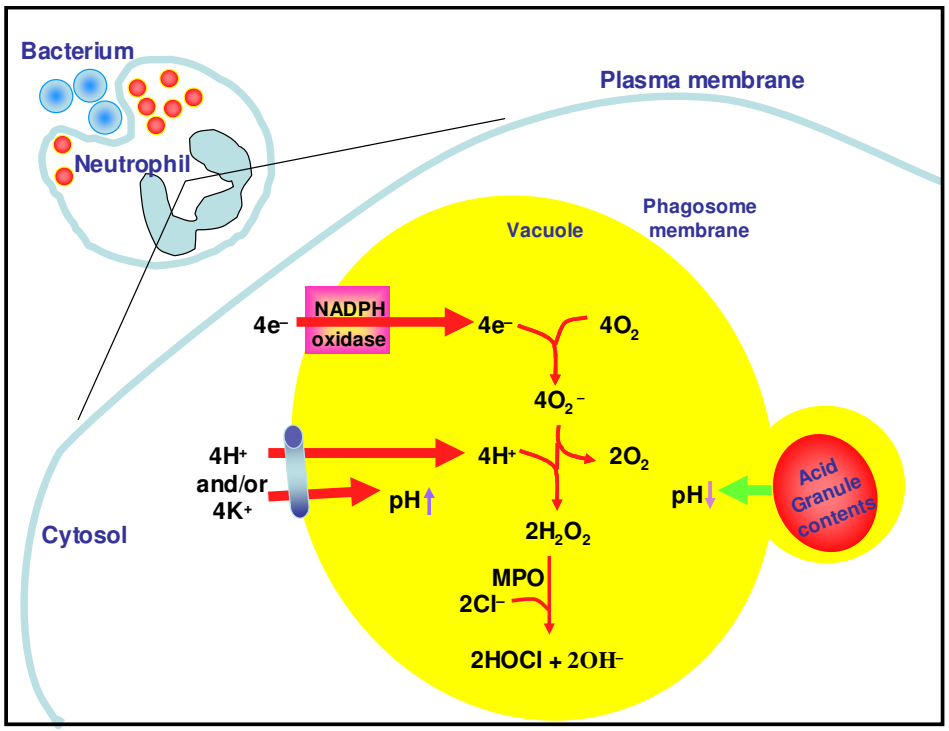

Figure 1. Phagocytose of bacteria and respiratory burst in the polynucleaire neutrophils

azurophil granules to produce hypochlorous acid (ClO^-), which is metabolized to hypochlorite and chlorine:

$$H_2O_2 + Cl^- + H^+ \xrightarrow{MPO} H_2O + HOCl$$

$$HOCl \longrightarrow H^+ + OCl^-$$

$$HOCl + Cl^- \longrightarrow Cl_2 + OH^-$$

H_2O_2 may be reduced to a very toxic compound, hydroxyl radical ($OH^\bullet$):

$$Fe^{2+} + H_2O_2 \longrightarrow Fe^{3+} + OH^- + OH^\bullet$$

$OH^\bullet$ is a powerful one-electron oxidant capable of abstracting electrons from a large variety of compounds with the formation of a new radical, which can oxidize other substances:

$$OH^\bullet + R \longrightarrow OH^- + R^\bullet$$

Hydroxyl radical and hypochlorite are the most powerful component involved in microbicidal and cytotoxic reactions. HOCl is about 100 to 1000 times more effective than H_2O_2. HOCl may react with amines ($R\text{-}NH_2$) to produce chloramines (R-NHCl), which are milder and longer lived oxidants than HOCl:

$$HOCl + R\text{-}NH2 \longrightarrow R\text{-}NHCl + H_2O$$

Singlet oxygen ($^1O_2$) is a dioxygen molecule which possesses a normal number of electrons but one of the unpaired electrons is lifted to a higher orbit with an inversion of spin. $^1O_2$ is produced by the reaction between H_2O_2 and hypochlorite:

$$H_2O_2 + OCl^- \longrightarrow {}^1O_2 + H_2O_2 + Cl^-$$

Light is emitted when the electrons relax into the ground state and can be measured by chemiluminescence. $^1O_2$ may react with a number of biological molecules, including membrane lipids, to initiate peroxidation.

ROS are involved in a variety of pathological conditions and are highly toxic for producing cells. Neutrophils have developed ROS scanvengers, e.g. catalase, glutathione and ascorbate.

H_2O_2 is stable and uncharged, it can cross cell membrane freely and can be destroyed by catalase or Glutathione peroxidase (GSH-PO):

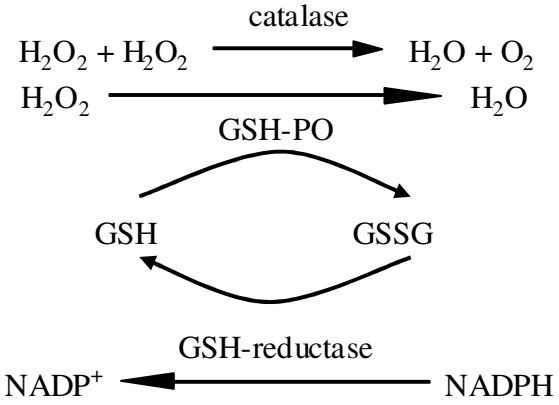

1.2 Electron transfer and compensation of charges mechanism

The NADPH oxidase catalyzes the production of superoxide by electron transfer from NADPH to molecular oxygen. Gp91^{phox}, containing the FAD and NADPH binding sites, is the catalytic center of this enzyme. It is generally believed that the transfer of electrons from NADPH to molecular oxygen occurs in two steps (Henderson et al. 1996). First, electrons are transferred from NADPH to the oxidized FAD moiety of cytochrome b_{558}. The second electron transfer step is from reduced FAD vie haems to oxygen. In this step, FAD semiquinone (FAD$^{\bullet}$) is generated and the electron is passed from inner to outer haem, then to oxygen forming superoxide (Cross et al. 2004). Electron-transfer from NADPH to FAD is dependent on p67^{phox}, but not p47^{phox}. In contrast, the electron transfer from FAD to oxygen via haems is dependent on p47^{phox} (Cross et al. 1994; Nisimoto et al. 1999). The first step of reaction can be monitored with artificial electron acceptors, such as iodonitrotetrazolium (INT), which can accept electrons directly from FADH and bypass the second step of reaction (Cross et al. 1994). A point mutation (Arg54Ser) in gp91^{phox} found in an X$^+$-CGD, appears to mainly affect the haem moiety of cytochrome b_{558}, which retains the capacity to reduce INT, but not superoxide (Cross et al. 1995*a*).

The oxidase is electrogenic, and its activation is accompanied by depolarization of the membrane. The charge across the vacuolar membrane is compensated mostly by protons (Henderson et al. 1987), gp91^{phox} may function as an essential part of the proton channel (Henderson et al. 1995). It is believed that neutrophils kill ingested microorganisms by the toxic ROS. While recently, the group of Segal demonstrated that killing activity of neutrophils is mediated through activation of cationic proteases by K^+ flux and the large-conductance Ca^{2+}-activated K^+ channel is essential for innate immunity (Reeves et al.

2002; Ahluwalia et al. 2004). Based on the finding that the inhibition of proton channel does not block the NADPH oxidase, K^+ flux was demonstrated to account for about 6% of the compensating charge. Indeed the superoxide anions will serve to activate the entry of K^+ flux, increasing the local ionic strength responsible for the liberation of cationic proteases (cathepsin G, elastase) from the internal membranes of phagolysosomes. These proteases will be the direct bactericidal agents.

More recently, the group of Ligeti indicated that both electrophysiological charges (deplorization and consequent ion movements) and the chemical effect of ROS play a significant role in the killing of certain pathogens (Rada et al. 2004).

2. NADPH oxidase

NADPH oxidase is a multicomponent complex, composed of a membranous component flavocytochrome b_{558}, and cytosolic proteins $p47^{phox}$, $p67^{phox}$, and $p40^{phox}$ (*phox* for *ph*agocytic *ox*idase) and two small GTPase, Rac2 and Rap1A (Table 1). In unstimulated cells, the NADPH oxidase components are segregated into membranes and cytosolic locations. $p40^{phox}$, $p47^{phox}$ and $p67^{phox}$ associate with a 1:1:1 stoichiometry in the cytosol (Groemping et al. 2005). Rac2 is located in the cytoplasm binding to Rho-GDI (GDP dissociation inhibitor). Rap1A is in the membranes from which it can be copurified with cytochrome b_{558} (Quinn et al. 1992, Quinn et al. 1995). Upon activation, a series of protein–protein and protein-lipid interactions occur. Both $p47^{phox}$ (Segal et al. 1985) and $p67^{phox}$ (Dusi et al. 1993) are phosphorylated and, along with $p47^{phox}$, translocate to membrane-bound cytochrome b_{558}. Rac2 binds guanosine triphosphate (GTP) and migrate to the membrane independently of $p67^{phox}$-$p47^{phox}$ complex. The activated NADPH oxidase transfers electrons from cytosolic NADPH to external molecular oxygen (Figure 2).

2.1 Cytochrome b_{558}

Segal and Jones identified for the first time a non-mitochondrial cytochrome *b* system in phagocytic vacuoles of human granulocytes (Segal et al. 1978). In human this b-type cytochrome was only found in professional phagocytic cells, like neutrophils, monocytes, macrophages, and eosinophils (Segal et al. 1981). This molecule was referred to as cytochrome b_{558} as the result of an absorbance maximum of the α band near 558 nm (Cross et al. 1984) or cytochrome b_{-245} because of its unusually low reduction midpoint potential of –245 mV (Jesaitis 1995). Cytochrome b_{558} is a membrane-bound heterodimeric protein consisting of two subunits: a glycosylated heavy chain ($gp91^{phox}$, β-subunit or Nox2) and a light, nonglycosylated polypeptide ($p22^{phox}$, α-subunit) (Parkos et al. 1987) (Table 1). These two subunits are in a 1:1 stoichiometry (Huang et al. 1995; Wallach et al. 1996). Most of the cytochrome b_{558} is associated with the specific granules and a small fraction (10-20%) is present in the plasma membrane of resting neutrophils (Borregaard et al. 1983). Upon activation, specific granules fuse with the plasma membrane at the site of the developing phagosome and respiratory burst (Morel et al. 1985). Spectrophotometric and redox potential measurements demonstrated that flavocytochrome b_{558} is a multi-haem protein with two distinct mid-potentials of -225 mV and -265 mV at pH 7.0 (Quinn et al. 1992*a*; Cross et al. 1995*b*). Flavocytochrome b_{558} contains all the catalytic machinery for catalyzing the

production of superoxide from oxygen and NADPH. The redox co-factors (FAD and haem *b*) and the binding sites for NADPH are confined to the gp91^{phox} (Vignais 2002).

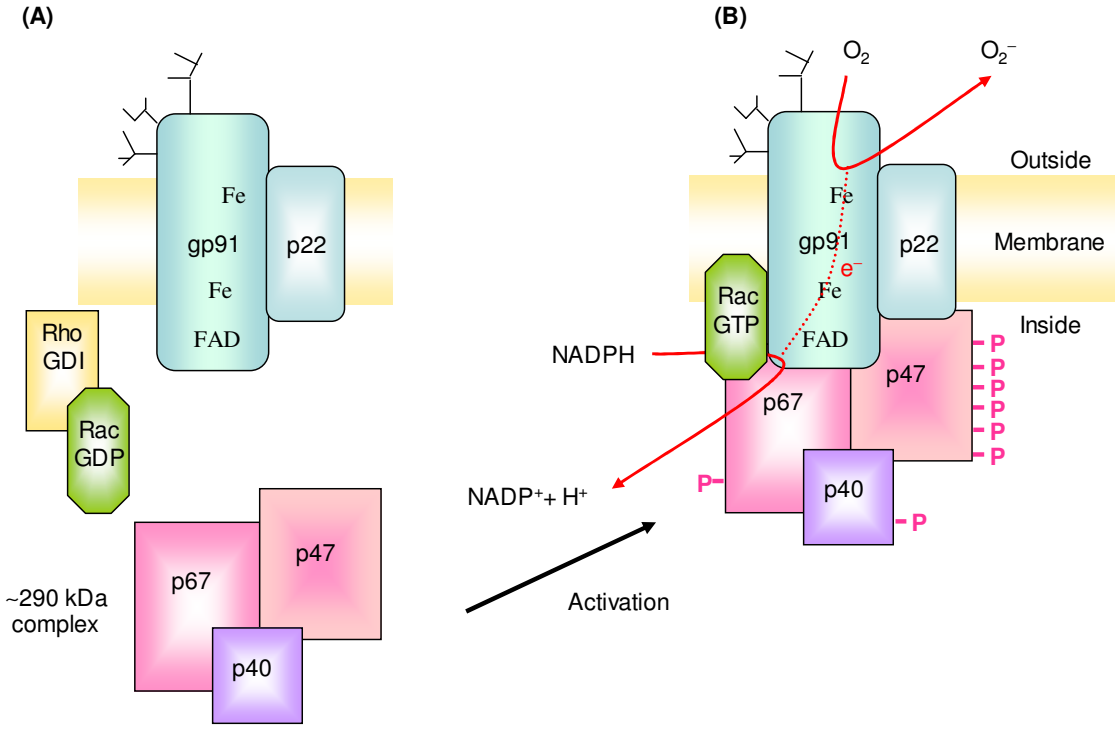

Figure 2. A model of phagocyte NADPH oxidase activation ('respiratory burst') (Heyworth et al. 2003). (A) In its resting state the oxidase is composed of dissociated membrane-bound and cytosolic protein components. (B) Upon activation p47^{phox}, p67^{phox} and p40^{phox} become stably associated with the plasma membrane. In a manner that is not yet fully understood, binding of the cytosolic components activates the flavocytochrome to catalyze the transfer of electrons from NADPH to oxygen, via the flavin and heme redox centers in gp91^{phox}, to form O_2.

- The gp91^{phox} subunit is encoded by *CYBB* gene located on the short arm of the X chromosome at locus Xp21.1 (Royer-Pokora et al. 1986). The *CYBB* gene contains 13 exons spanning 30 kb of genomic DNA (Orkin 1989; Hossle et al. 1993). Gp91^{phox}, containing 570 amino acid residues, has two major domains, the hydrophobic N-terminal domain containing six transmembrane α-helices (1-288 residues) which is important for anchoring the molecule in the plasma membrane and for interacting with the α subunit, and the hydrophilic C-terminal cytosolic portion containing the FAD and NADPH binding sites (289-570 residues) (Figure 3).

- The p22^{phox} contains 195 amino acid residues. This small subunit of cytochrome b_{558} is encoded by *CYBA* gene located in the chromosome 16 (16q24) (Dinauer et al. 1990). The mRNA expression of p22^{phox} was demonstrated to be ubiquitous. The primary structure suggests two membrane spanning domains in the N-terminus and the C-terminal cytosolic tail containing a strategic proline residue at 156 (Figure 3). The proline-rich region (^{156}PPRPP^{160}

Table 1 Properties of the phagocyte NADPH oxidase complex (Thrasher et al. 2000; Cross et al. 2004)

Component	Nox2 (gp91*phox*)	p22*phox*	p67*phox*	p47*phox*	p40*phox*	p21Rac2
Genetic locus	*CYBB*	*CYBA*	*NCF-2*	*NCF-1*		
Chromosomal location	Xp21.1	16q24	1q25	7q11.23	22q13.1	22q12
Gene/mRNA size	30 kb/4.7 kb	8.5 kb/0.8 kb	15.2 kb/1.4 kb	37 kb/2.4 kb	18 kb/1.2 kb	18 kb/1.5 kb
Exon number	13	6	16	11	10	7
Amino acids	570	195	526	390	339	192
Molecular weight:						
Predicted	65,338 Da	20,959 Da	59,735 Da	44,684 Da	30,039 Da	21,429 Da
By-SDS PAGE	~ 90 kDa	22 kDa	67 kDa	47 kDa		22 kDa
glycosylation	Yes	No	No	No	No	No
***p*I**	9.26	10.1	6.12	9.58	7.28	7.87
Phosphorylation	No	Minor	Minor	Yes	Yes	?
Location inPMN						
Resting	Specific granules and plasma membrane		Cytosol	Mainly cytosol	Cytosol	Cytosol
Stimulated	Plasma membrane and phagosome		Membrane	Membrane	Membrane	Membrane
Abundance pmol/10^6 cells (cytosol conc.)	1.0-2.0	1.0-2.0	1.0 (460 nM)	6.0 (2750 nM)	1.0 (460 nM)	2.6 (1200 nM)
Tissue specificity	Myeloid. Low levels in mesangial cells and some B-lymphocytes	Ubiquitous	Myeloid	Myeloid	Myeloid	

and ^{177}GGPPGGP^{183}) binds to the N-terminal SH3 domain of p47^{phox}, which seems to play a dominant role in the oxidase assembly process (Leto et al. 1994). P22^{phox} is not the redox center for the NADPH oxidase, but it is indispensable for the maturation of gp91^{phox} in myeloid cell lines. However, some authors proposed four transmembrane regions of the N-terminus of p22^{phox} (Figure 3) (Heyworth et al. 2003).

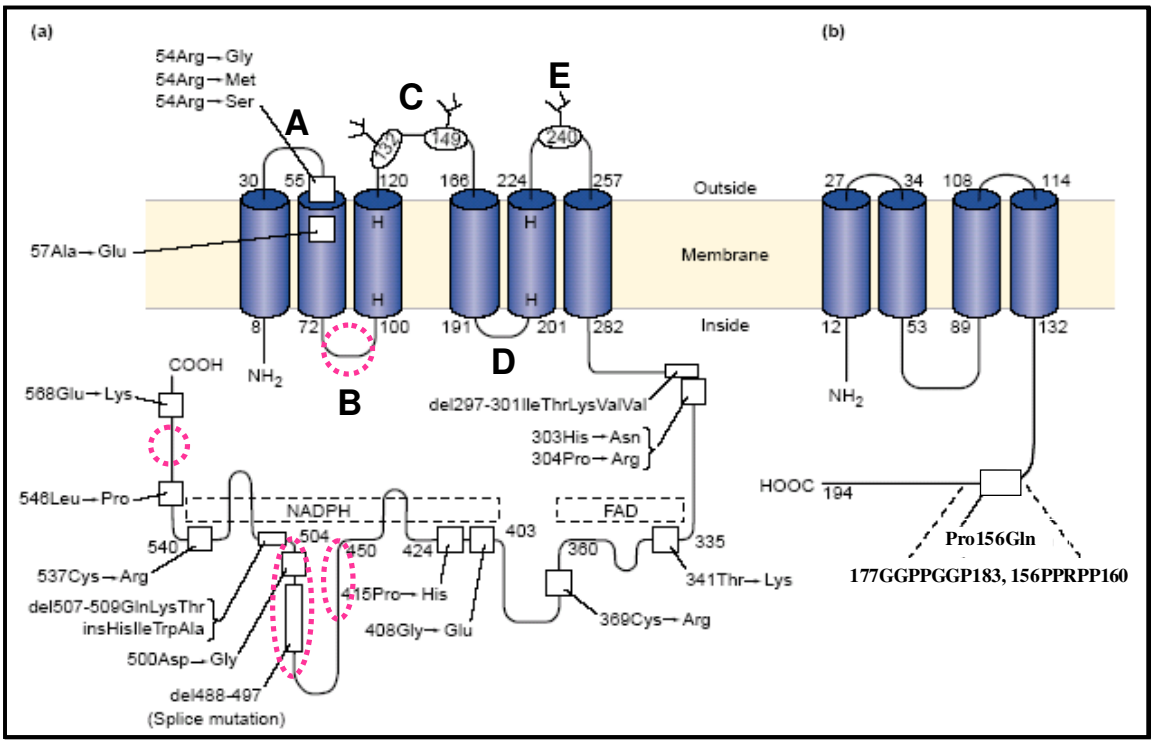

Figure 3. Model of cytochrome b_{558} (Heyworth et al. 2003). Mutations causing X^+ (16 mutations) and $A22^+$ (one mutation) forms of CGD on membrane-spanning models of gp91^{phox} and p22^{phox}. (a) Gp91^{phox} contains 6 transmembrane domains, the four heme-binding histidines (residues 101, 115, 209 and 222) are shown in the third and fifth membrane-spanning domains. Glycosylated asparagines are identified by their residue numbers (132, 149 and 240) and the approximate position of the FAD and NADPH-binding domains are indicated by dashed boxes. Open rose-circle indicate the potential binding sites for cytosolic factors. (b) P22^{phox} contains 4 transmembrane regions and a C-terminal cytosolic region, containing a proline-rich region (^{156}PPRPP^{160} and ^{177}GGPPGGP^{183}). The single mutation in p22^{phox} known to cause an $A22^+$ form of CGD, occurs in the SH3-binding proline-rich domain.

2.2 Cytosolic components of NADPH oxidase

▸ P47*phox* (NCF1, neutrophil cytosolic factor 1; NoxO2)

P47^{phox} comprising 390 amino acids, is encoded by the *NCF1* gene which is located on chromosome 7 (locus 7q11.23) (Lomax et al. 1989). P47^{phox} contains an N-terminal phox homology (PX) domain (residues 4-128), two SH3 domains (*S*rc *h*omology domain *3*) (residues 156-215 and 226-285), a region rich in serine residues (314-347), the potential phosphorylation sites, and a C-terminal proline-rich region (PRR) (residues 360-369) (Figure 4) (Takeya et al. 2003; Massenet et al. 2005). In resting neutrophil cytosol, an auto-inhibited

conformation of p47^{phox} is generated by the interactions between the SH3 domains with the PX region and the PRR domain. The PxxP motif (residues 73-76) in the PX domain and the N-terminal SH3 could bind to the membrane phosphoinositides and p22^{phox}, respectively (Leto et al. 1994; De Mendez et al. 1996; Hiroaki et al. 2001; Karathanassis et al. 2002).

Upon stimulation of neutrophils, p47^{phox} undergoes extensive phosphorylation which causes a conformational change (Figure 4). Phosphorylation of p47^{phox} is concentrated in a cluster of serine residues between Ser^{303} and Ser^{379} in the C-terminus. Eleven phosphorylation sites have been identified in its C-terminus (El Benna et al. 1994; Faust et al. 1995; El Benna et al. 1996; Inanami et al. 1998; Fontayne et al. 2002). Phosphorylation occurs in a sequential manner, Ser^{359} and Ser^{370} being phosphorylated prior to Ser^{303} and Ser^{304} (Johnson et al. 1998; Inanami et al. 1998). Mutagenesis study (Ser replaced by Ala or Glu) demonstrates that a negative electrostatic potential in Ser^{303} and Ser^{304} is absolutely required for the activity of p47^{phox} (Inanami et al. 1998).

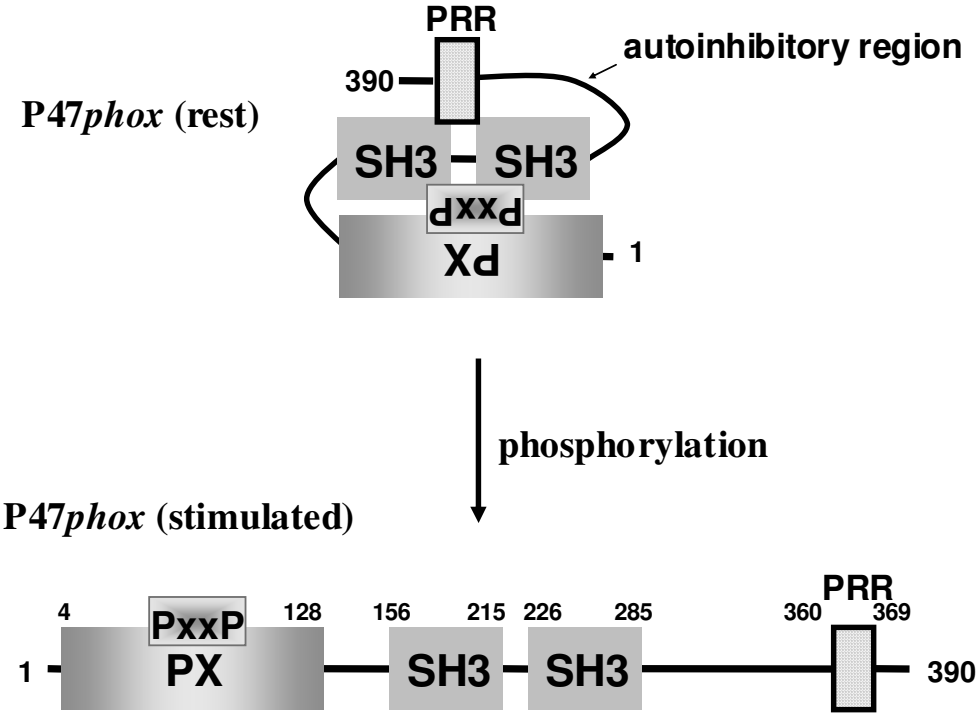

Figure 4. Structural model of p47*phox* (Takeya 2003). Both resting and activated configurations of p47^{phox} are shown with its functional domains.

P47^{phox} is essential for NADPH oxidase *in vivo*, but it is not absolutely required for superoxide production in the CFS assay (Freeman et al. 1996). Indeed full oxidase activity can be reconstituted *in vitro* without p47^{phox}, by increasing the concentration of Rac and p67^{phox}. By using atomic force microscopy (AFM), Paclet *et al.* found that p47^{phox} proceeded as a positive effector and increased the affinity of p67^{phox} for cytochrome b_{558} (Paclet et al. 2000). As the result, p47^{phox} is also known as NoxO (Nox organizer) (Cross et al. 2004).

Recently, a novel homolog of p47^{phox} (NoxO1 or p41), in which the auto-inhibitory domain and the PKC phosphorylation sites are absent, was discovered in the colon epithelium (Banfi et al. 2003; Geiszt et al. 2003*a*). Unlike p47^{phox}, NoxO1 co-localizes with Nox1 (a homologue of Nox2, abundantly expressed in the colon) (Suh et al. 1999) in the membranes

of resting cells and participates to the constitutive activity of Nox1 (Cheng et al. 2004).

▸ P67*phox* (NCF2, neutrophil cytosolic factor 2; NoxA2)

P67^{phox} was initially identified as a missing neutrophil cytosolic factor 2 (*NCF2*) in patients with autosomal CGD (Volpp et al. 1988; Nunoi et al. 1988). P67^{phox} is a 526-amino-acid protein with a molecular mass of 59.8 kDa, which contains an N-terminal TPR (*t*etraco*p*eptide *r*epeat), two SH3 domains (residues 240-299 and 457-518), a PB1 domain (residues 338-428), and an activation domain (residues 199-213) (Figure 5) (Takeya et al. 2003; Groemping et al. 2005). TPR domains are known to promote protein-protein interactions. The TPR domain of p67^{phox} functions as a Rac target (Koga et al. 1999). In addition, this motif may also bind NADPH and exhibit weak dehydrogenase activity (Dang et al. 1999). PB1 domains are novel protein modules capable of binding to target proteins that contain PC motifs (Ito et al. 2001). This motif has been named after its occurrence in the *p*hagocytic oxidase and *B*em 1. The PB1 in p67^{phox} forms a heterodimer with the PC domain of p40^{phox} (Kuribayashi et al. 2002). During oxidase activation, p67^{phox} is phosphorylated and the major phosphorylation site is Thr^{233} (Forbes et al. 1999). The activation domain of p67^{phox} has been demonstrated to be absolutely required for superoxide generation in CFS assay (Han et al. 1998). This domain appears to participate in the regulation of electron transfer and interact directly with cytochrome b_{558} (Nisimoto et al. 1999). Consequently, p67^{phox} has been called NoxA (Nox activator).

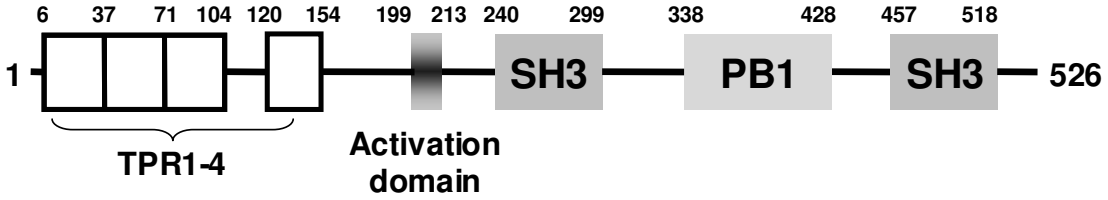

Figure 5. Structural model of p67*phox* (Takeya 2003). Functional domains are shown.

The study of the complementation of p67^{phox}-deficient CGD mutants in a reconstituted CFS assay confirmed that p67^{phox} is the critical cytosolic component of oxidase activation (Vergnaud et al. 2000). However, the membrane-translocation of p67^{phox} is absolutely dependent on the presence of p47^{phox} *in vivo* (Heyworth et al. 1991). The atomic force microscopy study indicated that p47^{phox} enhanced the affinity of the binding sites of p67^{phox} and Rac2 for cytochrome b_{558} in a CFS assay (Paclet et al. 2000).

A homologue of p67^{phox} has been discovered and termed as NoxA1 (Nox activating protein 1 or p51) (Banfi et al. 2003; Geiszt et al. 2003*a*). NoxA1 is highly expressed in pancreas and colon (Cheng et al. 2004). In transfected HEK293 cells, NoxO1 and NoxA1 activate Nox1 without the need for agonist activation. NoxO1 and NoxA1 are capable of replacing their corresponding classical homologues (p67^{phox} and p47^{phox}) in the activation process of Nox2. In contrast to p67^{phox}, its homologue NoxO1 is incapable of interacting with p40^{phox}, indicating that p40^{phox} is not involved in NoxO1-dependent regulation of Nox oxidases (Takeya et al. 2003).

Rac

Based on the use of purified recombinant proteins in CFS assays, a small GTP-dependent protein (G protein) was identified as Rac1 (Abo et al. 1991) and Rac2 (Knaus et al. 1991). Both are geranylgeranylated at the C-terminus, which facilitates their association with plasma membranes. Two Rac isoforms are 92% identical in their 192 amino acid residues. Rac2 is the predominant form in neutrophils, but Rac1 can restore the NADPH oxidase activity in Rac2 deficient cells (Gu et al. 2001). Rac2, a hemopoietic specific member of the small RhoGTPases family, regulates neutrophil chemotaxis, superoxide production, and myeloid colony formation through multiple distinct effector pathways (Carstanjen et al. 2005).

Under resting conditions, Rac is located in the cytosol and associated with RhoGDI (GDP dissociation inhibitor), which maintains it in its inactive form (Pick et al. 1993). Crystal structure study indicated that residues Tyr^{64}, Arg^{66}, His^{103}, and His^{104} of Rac1 are implicated in the interaction with RhoGDI and the hydrophobic interactions involving Leu^{67} and Leu^{70} of Rac1 contribute to the stability of Rac1-RhoGDI complex (Grizot et al. 2001*a*). Appropriate stimuli induce its dissociation from GDI, allowing membrane translocation independent of the other oxidase subunits and its interaction with $p67^{phox}$ (Heyworth et al. 1994; Koga et al. 1999). The exchange of GDP against GTP is catalyzed by GEP proteins (GDP/GTP exchange factors).

P40*phox*

$P40^{phox}$ was discovered through co-purification with $p67^{phox}$ (Someya et al. 1993). It comprises 339 amino acids with a molecular mass of 39.0 kDa. $P40^{phox}$ contains an N-terminal PX domain, an SH3 domain and a PB1 domain (previously described as PC domain and represents *p*hox and *C*dc24) (Groemping et al. 2005) (Figure 6). It interacts with $p67^{phox}$ via its PB1 domain, and its SH3 domain has been suggested to interact with the PRR of $p47^{phox}$ (Grizot et al. 2001*b*). The overall function of $p40^{phox}$ is very controversial, it has been described as both activator and inhibitor (Tsunawaki et al. 1996; Sathyamoorthy et al. 1997; Vergnaud et al. 2000).

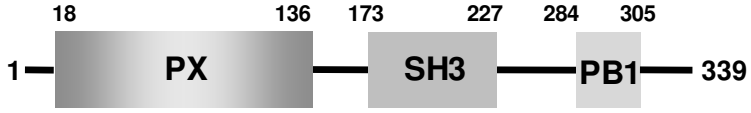

Figure 6. Structural model of p40*phox* (Lapouge 2002). Functional domains are shown.

2.3 Rap1A

Rap1A is a small G protein, belonging to the rab family and discovered through its association with cytochrome b_{558} during its purification (Quinn et al. 1989; Quinn et al. 1992*b*). In neutrophils, Rap1A is activated by several signaling pathway, independently of both the functional NADPH oxidase complex and the presence of cytochrome b_{558} (Vignais 2002). Its exact role in the NADPH oxidase activation has not been clear (Quinn et al. 2004).
Rap1A has been shown to bind specifically to cytochrome b_{558} with a one-to-one stoichiometry. In neutrophils, Rap1A becomes phosphorylated by the cAMP-dependent kinase PKA (Quilliam et al. 1991; Quinn et al. 1992*c*). A serine residue (Ser^{180}) at the

C-terminus of Rap1A has been identified as a site of phosphorylation by PKA. Phosphorylation of Rap1A abrogates its interaction with cytochrome b_{558} (Bokoch et al. 1991). It is possible that phosphorylation of Rap1A can regulate the deactivation of the NADPH oxidase.

3. Gp91*phox* (β-subunit, Nox2)

Sequence alignment of Nox2 with members of the ferredoxine-$NADP^+$ reductase family (FNR) demonstrates the presence of six transmembrane α-helices in the N-terminal hydrophobic region, four cytosolic regions, the ^{1}MGNWVAVNEGL^{11} sequence, the B loop ^{70}PVCRNLLSFLRGSSACCSTRIRRQLDRNLTFHK^{102}, the D loop ^{191}TSSTKTIRRS^{200}, and a C-terminal region containing binding sites for FAD, NADPH (Figure 7) (Vignais 2002; Paclet et al. 2004). Gp91^{phox} is the catalytic center that transfers the electrons from intracellular NADPH to extracellular O_2. It contains two nonidentical haems (Segal et al. 1992; Yu et al. 1998).

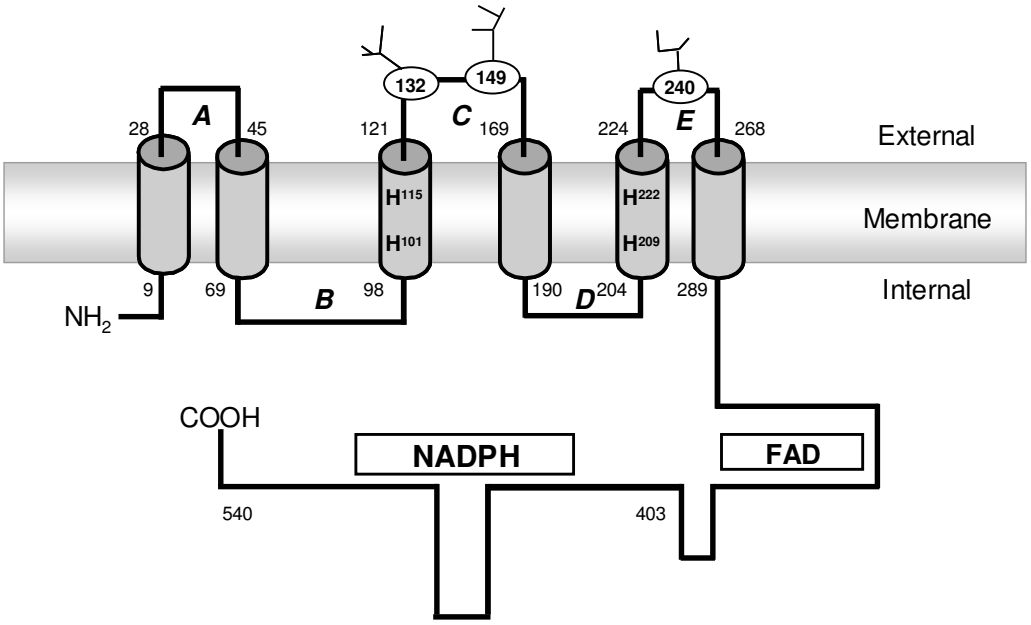

Figure 7. Structure of gp91*phox* (Vignais 2002; Cross et al. 2004). The N-terminal six transmembrane helices and the C-terminal cytosolic region, containing the potential binding sites for FAD and NADPH.

3.1 Haem-binding sites

Each putative helice III and V contains one pair of histidine residues (101/115 and 209/222) which are supposed to be coordinated with two haem prosthetic groups (Vignais 2002). In this model (Figure 8), one haem is positioned closely to the cytosolic space (101:209), near the FAD-binding sites. The second haem is close to the extracellular space. This bis-haem model is consistent with their function: the transfer of electrons from cytosolic NADPH (via FAD) across the vacuole membrane to molecular O_2. Similar haem arrangement (294:364 and 308:378) has been reported in FRE1 protein of the iron reductase, homologous to gp91^{phox} (Finegold et al. 1996). Replacing histidine residues with alanine in FRE1 (H294A, H308A, H364A, H378A) resulted in a deficiency in reductase activity and haem

spectrophotometric absorption, suggesting that these histidine residues are involved in the binding of haems.

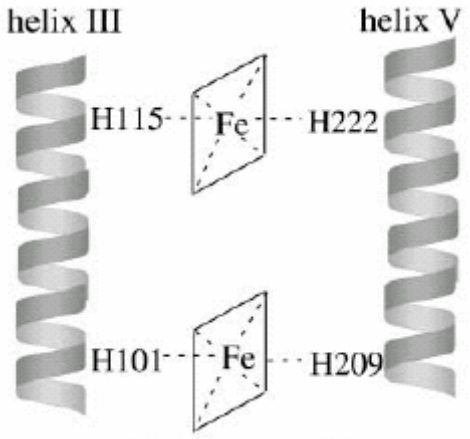

Figure 8. Model of Bis-haem in gp91^{phox}, in which two pairs of histidine residues (His^{101} and His^{209}; His^{115} and His^{222}) are involved in the ligand (Vignais 2002).

Gp91^{phox} possesses seven histidine residues (101, 111, 115, 119, 209, 210, 222) localized within transmembrane domain III and V. Site-directed mutegenesis study demonstrated that His^{101}, His^{115}, His^{209}, and His^{222} are necessary for coordinating the two heme prosthetic groups of phagocyte flavocytochrome *b* (Figure 7) (Biberstine-Kinkade et al. 2001). Missense mutations in any of these residues (His^{101}, His^{115}, His^{209} and His^{222}) have been associated with a number of X^0-CGD or X^--CGD (Heyworth et al. 2001). This suggests that the haem-incorporation is associated with the maturation and/or the stability of gp91^{phox} in neutrophils.

The invariant histidine residue (His^{94}) in p22^{phox} had been proposed to as one of the axial ligands to one of two haems (De Boer et al. 1992; Park et al. 1994; Foubert et al. 2001). Definitive evidence for the localization of the two haems in gp91^{phox} stems from site-directed mutagenesis in the His^{94} of p22^{phox}, suggesting that this residue is not involved in haem binding (Biberstine-Kinkade et al. 2002). The incorporation of haems was found to play a crucial role in the formation of the gp91^{phox}-p22^{phox} heterodimer (Yu et al. 1997; DeLeo et al. 2000).

3.2 FAD-binding site

The idea that NADPH oxidase contains FAD prosthetic group is supported by several evidences. FAD enhanced (Babior 1977), and its analogue 5-deaza-FAD inhibited, the activity of the solubilized oxidase (Light et al. 1981). The NADPH oxidase activity can be inhibited by DPI (diphenylene iodonium), a potent flavoprotein inhibitor (Cross et al. 1987). Electron spin resonance studies demonstrated that a semi-quinone form of FAD was presented in membranes of the activated neutrophils (Kakinuma et al. 1986). FAD is essential for the NADPH oxidase activity in a CFS assay with purified cytochrome b_{558} and neutrophil cytosol (Sumimoto et al. 1992) or recombinant proteins (Rotrosen et al. 1992). Purified cytochrome b_{558} required FAD to be functional, suggesting that cytochrome b_{558} is an FAD-binding flavoprotein (Sumimoto et al. 1992).

The concentration of FAD in the plasma membranes from normal neutrophils is similar to those from membranes of autosomal recessive CGD (AR-CGD) neutrophils, but is approximately 3-time higher than those from X-CGD neutrophils (Segal et al. 1992). The ratio of FAD:haem is roughly 1:2 in membranes from unstimulated and stimulated control AR-CGD neutrophils (Bellavite et al. 1983; Segal et al. 1992). This provides strong evidence that cytochrome b_{558} is an FAD-binding flavocytochrome.

The identification of the β subunit as a flavoprotein was supported by the finding of amino acid sequence homology in the conserved nucleotide-binding domains in FNR family (ferredoxin-NADP reductase). Sequence alignment of gp91^{phox} with the FAD-binding regions of several flavoproteins suggested that gp91^{phox} residues 214-246, 335-345, and 350-360 are involved in FAD-binding (Segal et al. 1992; Sumimoto et al. 1992) (Figure 7). Recent information indicates that residues 214-246 are located in the extracellular loop (Wallach et al. 1997; Burritt et al. 2001). The motif containing residues ^{338}HPFT^{341} was proposed to interact with flavin. It is strictly conserved in porcine and mouse gp91^{phox}. The importance of His^{338} for FAD-binding is also supported by a rare X^{-}-CGD resulting from a missense mutation His338Tyr, in which FAD was completely depleted in the mutated gp91^{phox} associated with a diminished expression (Yoshida et al. 1998). This indicated that His^{338} is a critical residue for FAD incorporation into gp91^{phox}and that this incorporation is directly linked with the gp91^{phox} stability. Other mutations in the potential FAD-binding residues, Leu342Gln, Ser344Phe, and Gly359Arg cause X^{0}-CGD (Heyworth et al. 2001). However, Pro339His missense mutation resulted to an X^{-}-CGD, and Thr341Lys led to an X^{+}-CGD (Leusen et al. 1999). This confirms that FAD incorporation in gp91^{phox} maybe involved in protein stabilization during the biosynthesis of cytochrome b_{558}. In the three-dimensional model of the C-terminus of gp91^{phox}, Arg^{355} is proposed to lie between the adenine and the nicotinamide halves and interacts equally with both phosphates (Taylor et al. 1993).

The synthetic peptide corresponding to residues 329-350 has no inhibition in NADPH oxidase activity in a CFS assay, suggesting that the FAD-binding region is inside the molecule (Park et al. 1997). A recently study showed that binding of FAD to cytochrome b_{558} is facilitated during activation of phagocyte NADPH oxidase (Hashida et al. 2004).

3.3 NADPH-binding site

A flavoprotein (65-67 kDa) was found to bind NADPH in the neutrophil membranes by radio-reactive and photoaffinity studies (Doussière et al. 1986; Kakinuma et al. 1987). Based on photolabeling and affinity labeling experiments, the NADPH-binding sites of flavocytochrome b_{558} have been revealed in gp91^{phox} (Ravel et al. 1991; Segal et al. 1992; Doussière et al. 1993; Ravel et al. 1993). In NADP(H)-dependent flavoenzyme, the NADP(H)-binding domain is expected to be localized in a relatively C-terminal portion from the FAD-binding region. Based on comparison of the amino acid sequences of gp91^{phox} , FNR and related flavoproteins, four regions are considered to be potential NADPH-binding domains in the C-terminus of gp91^{phox} (Figure 7, 9) (Rotrosen et al. 1992). Two of them are particularly conserved. The first one is residues ^{405}MLVGAGIGVTPF^{416} containing the Gly-X-Gly-X-X-Pro motif, which is involved in the binding of the pyrophosphate moiety of NADPH in FNR family. The importance of this domain is supported by the Gly408Glu

		Pyrophosphate														Ribose							Adenine						Nicotinamide							
Homo sapiens	Nox2 (gp91phox)	405	M	L	V	G	A	G	I	G	V	T	P	F	416	442	Y	W	L	C	R	446	504	G	L	K	Q	507	535	F	L	C	G	P	E	540
	Nox-1	399	V	L	V	G	A	G	I	G	V	T	P	F	410		-	-	-	-	-		498	G	L	K	Q	501	480	F	L	C	G	P	R	485
	Nox-3	403	V	C	V	A	A	G	I	G	V	T	P	F	414	440	Y	W	I	C	R	444	502	G	L	K	Q	505	533	F	F	C	G	P	K	538
	Nox-4	427	L	C	V	A	G	G	I	G	V	T	P	F	438	460	I	W	V	C	R	464	514	A	L	N	S	520	545	F	C	C	G	P	N	550
	Nox-5	385	V	L	I	G	A	G	I	G	I	T	P	F	396	437	I	W	I	N	R	441	508	G	L	Q	T	511	538	F	F	C	G	S	P	543
	Duox 1	1384	V	L	V	G	G	G	I	G	V	T	P	F	1395	1420	I	W	V	T	R	1424	1486	G	L	R	S	1489	1508	F	S	C	G	P	P	1513
	Duox 2	1381	V	L	V	G	G	G	I	G	V	T	P	F	1392	1417	I	W	V	T	R	1421	1483	G	L	R	S	1486	1515	F	S	C	G	P	P	1520
Rattus	gp91-phox	405	M	L	V	G	A	G	I	G	V	T	P	F	416	442	Y	W	L	C	R	446	504	G	L	K	Q	507	535	F	L	C	G	P	E	540
Mus musculus	gp91-phox	405	M	L	V	G	A	G	I	G	V	T	P	F	416	442	Y	W	L	C	R	446	504	G	L	K	Q	507	535	F	L	C	G	P	E	540
Rattus norvegicus	Endothelial type gp91-phox	405	M	L	V	G	A	G	I	G	V	T	P	S	416	442	Y	W	L	C	R	446	504	G	L	K	Q	507	535	F	L	C	G	P	E	540
pig	NADPH oxidase heavy chain subunit	303	M	L	V	G	A	G	I	G	V	T	P	F	314	340	Y	W	L	C	R	344	402	G	L	K	Q	405	433	F	L	C	G	P	E	438
Oryctolagus cuniculus	gp91-phox	405	M	L	V	G	A	G	I	G	V	T	P	F	416	442	Y	W	L	C	R	446	504	G	L	K	Q	507	535	F	L	C	G	P	E	540
Bos taurus	NADPH oxidase heavy chain subunit	405	M	L	V	G	A	G	I	G	V	T	P	F	416	442	Y	W	L	C	R	446	504	G	L	K	Q	507	535	F	L	C	G	P	E	540
Tursiops truncatus	gp91-phox	405	M	L	V	G	A	G	I	G	V	T	P	F	416	442	Y	W	L	C	R	446	503	G	L	K	Q	506	534	F	L	C	G	P	E	539
Dictyostelium discoideum	NADPH oxidase	357	I	L	V	G	A	G	I	G	V	T	P	F	368	395	Y	W	I	C	R	399	453	G	F	T	T	456	484	F	F	C	G	P	K	489
Emericella nidulans	NADPH oxidase	370	V	L	I	G	T	G	I	G	V	T	P	W	381	407	I	W	V	C	K	411	475	E	L	K	S	478	518	Y	F	C	G	P	N	523
Rice	rboh A-rice	390	L	L	V	G	L	G	I	G	A	T	P	F	401	460	Y	W	V	T	R	464	526	G	T	K	V	529	557	F	Y	C	G	A	P	562
Nicotiana tabacum	NADPH oxidase	761	L	L	V	G	L	G	I	G	A	T	P	F	772	832	Y	W	V	T	R	836	898	G	T	R	V	901	929	F	Y	C	G	A	P	934

Figure 9. Amino acid sequence alignment of the potential NADPH-binding sites of Nox2 in the human Nox/Duox and Nox2 family.

substitution which disturbed the electron transfer in solubilized plasma membranes from an X^+-CGD patient (Leusen et al. 2000). The photoaffinity study using 2-azido-$NADP^+$ demonstrated that the Pro415His mutation found in an X^+-CGD (Dinauer et al. 1989) disturbed the NADPH-binding (Segal et al. 1992). Introduction of a mutation in proline of Nox3 (Pro413His), one homologue of $gp91^{phox}$, resulted to an inactive Nox3 (Ueno et al. 2005), supporting that this proline is particularly important for Nox activity.

The second highly conserved domain of NADPH in FNR is the Cys-Gly dipeptide ($^{537}CG^{538}$), which is located in the nicotinamide-binding site (Sumimoto et al. 1992; Segal et al. 1992). An X^+-CGD originates from the missense mutation Cys537Arg (Rae et al. 1998), pointed out that this residue is absolutely necessary for NADPH oxidase activity. The sequence of residues 442-446 was considered to be a binding site for the ribose of NADPH (Rotrosen et al. 1992). This domain is similar in enzymes closely related to cytochrome P-450 reductase, but slightly similar to FNR family members (Sumimoto et al. 1992). Based on a peptide inhibitory study, peptides corresponding to residues 441-450 and 434-455 of $gp91^{phox}$ inhibited superoxide generation in a CFS assay (Tsuchiya et al. 1999), suggesting that these peptides caused distortion of the NADPH binding site (residues 442-446).

Residues $^{504}GLKQ^{507}$ were considered to be the binding site for adenine of NADPH (Rotrosen et al. 1992; Vignais 2002). According to the 3D model of Taylor and Segal, this region is buried by residues 484-504 in the C-terminus of $gp91^{phox}$ (Figure 3) (Taylor et al. 1993). A new point mutation (Leu505Arg) located in this potential domain has been reported to lead an X^+-CGD (Stasia et al. 2005). The affinity for NADPH/NADH of this mutant is slightly lower than that of the wild type $gp91^{phox}$, indicating that this amino acid is not directly involved in the NADPH-binding process.

3.4 Glycosylation and maturation

$Gp91^{phox}$ contains 570 amino acids and its predicted molecular weight is 65,338 Da. Harper *et al.* was the first to find that the purified cytochrome b_{558} ran as a broad band in SDS-PAGE with an apparent Mr of 76-88 kDa due to its heavy glycosylation state (Harper et al. 1985). Subsequent researchs showed that the human neutrophil cytochrome b_{558} is a heterodimer of a heavily glycosylated polypeptide (Mr 91,000) with a polypeptide core of 50-kDa and an unglycosylated 22-kDa polypeptide (Parkos et al. 1987). This observation demonstrated that the large subunit contains large amounts of N-linked carbohydrate. Analysis of carbohydrate content of cytochrome b_{558} indicated that the majority are N-acetyl glucosamine and galactose, while minor sugars are mannose, glucose, fucose, and xylose (Harper et al. 1985).

There are five asparagine residues at position 97, 132, 149, 240, and 430 considered as potential N-linked glycosylated sites in $gp91^{phox}$ (Figure 7). Based on the site-directed mutagenesis approach (Asn replaced by Thr), only Asn^{132}, Asn^{149} and Asn^{240} were shown to be involved in the glycosylation events (Wallach et al. 1997). These Asn residues are partly conserved among mammals. For example, Asn^{132} and Asn^{149} are missing in $gp91^{phox}$ of mouse and dolphin (Bjorgvinsdottir et al. 1996). While Asn^{240} is absent in $gp91^{phox}$ of rabbit (Gauss et al. 2002). These can explain the different molecular mass of $gp91^{phox}$ observed in SDS-PAGE from different species, which corresponds to different levels of $gp91^{phox}$ glycosylation.

Porter *et al.* identified the precursor of gp91^{phox} (gp65) containing high mannose carbohydrate side chains in B cell lines from A22^{0}CGD patients (Porter et al. 1994). This indicates that the initial steps of oligosaccharide addition and processing occur in the absence of p22^{phox} within the endoplamic reticulum (Yu et al. 1997). Fully oligosaccharide side chains addition can be restored by transfection of p22^{phox} cDNA in A22^{0}-CGD B cells (Maly et al. 1993; Porter et al. 1994), indicating that the presence of p22^{phox} facilitates the glycosylation and stability of gp91^{phox}. The glycosylation of gp91^{phox} depends on the cellular types. For example, in gp91^{phox} transfected COS-7 cells, the majority of gp91^{phox} is under its gp65 precursor form (Yu et al. 1998; Maturana et al. 2002; Murillo et al. 2005; our observations). However, glycosylation is not a requirement for gp91^{phox} catalytic function (Paclet et al. 2000). In addition the glycosylation of gp91^{phox} seems to protect it against proteolytic degradation (Paclet et al. 2001).

3.5 Proton channel

The oxidase is electrogenic (Henderson et al. 1987). The electron current generated by the NADPH oxidase has been recorded in neutrophils by several groups (Schrenzel et al. 1998; Banfi et al. 1999; DeCoursey et al. 2000). A charge compensation is absolutely required for continuous NADPH oxidase function. A proton channel was reported to be associated with the NADPH oxidase activity. The idea that gp91^{phox} is a proton channel was supported by several experiments. CHO cells and undifferentiated HL-60 cells transfected with gp91^{phox} cDNA expressed H^+ channel activity related to the expression of gp91^{phox} (Henderson et al. 1995). Transfected CHO cells, expressing the N-terminal 230 amino acids of gp91^{phox}, exhibited an arachidonte-activable proton flux in response to an imposed proton motive force (Henderson et al. 1997) (Figure 7). No H^+ flux was observed in CHO cells expressing gp91^{phox} bearing point mutations on the histidine residues 111, 115, and 119, suggesting that theses residues are important for the ability of gp91^{phox} to function as a H^+ channel (Henderson et al. 1998).

However, cells from X-CGD patients displayed normal outward proton currents that could be up-regulated by physiological stimuli, suggesting that a proton channel distinct from gp91^{phox} was present in phagocytes (Banfi et al. 1999). In transfected HEK 293 cells, the mutation His115Leu-gp91^{phox} abolished both the gp91^{phox} characteristic absorbance peak at 558 nm and voltage-activated currents, indicating that haem-histidine ligands within gp91^{phox} modulate proton conduction by the NADPH oxidase (Maturana et al. 2001). Based on the electrphysiological and pharmacological characteristics, it is likely that there are different types of H^+ channels (Maturana et al. 2002). Gp91^{phox} was probably the low threshold channel associated with an active oxidase (Maturana et al. 2002).

On the contrary, DeCoursey had observed that the gp91^{phox} of NADPH oxidase was not the voltage-gated proton channel in phagocytes, but it helped (DeCoursey et al. 2001). However, there is a general consensus in the field regarding the existence of the H^+ conductance in phagocytes. Touret and Grinstein have proposed that it appears that gp91^{phox} is not the conductance entity, but it is equally obvious that the oxidase component plays a modulatory role on the conductance (Touret et al. 2002).

3.6 Homologues of Nox2

Recently, the research for non-phagocyte NADPH oxidase led to the discovery of two families of gp91^{phox} homologues, Nox (for *N*ADPH *ox*idase) and Duox (for *du*al *ox*idase) (Cross et al. 2004; Lambeth 2004) (Figure 10, Table 2). All the Nox family members contain a core structure consisting of six transmembrane domains (in which four haem-coordinating hisidine residues are located), and a C-terminal cytosolic region (which contains highly conserved binding sites for FAD and NADPH). Nox5, Duox1 and Duox2 are characterized by N-terminal extensions: 3 EF-hand domains in Nox5; 2 EF hand domains, an additional transmembrane region, and a peroxidase homology domain in Duox1/2 (Figure 10).

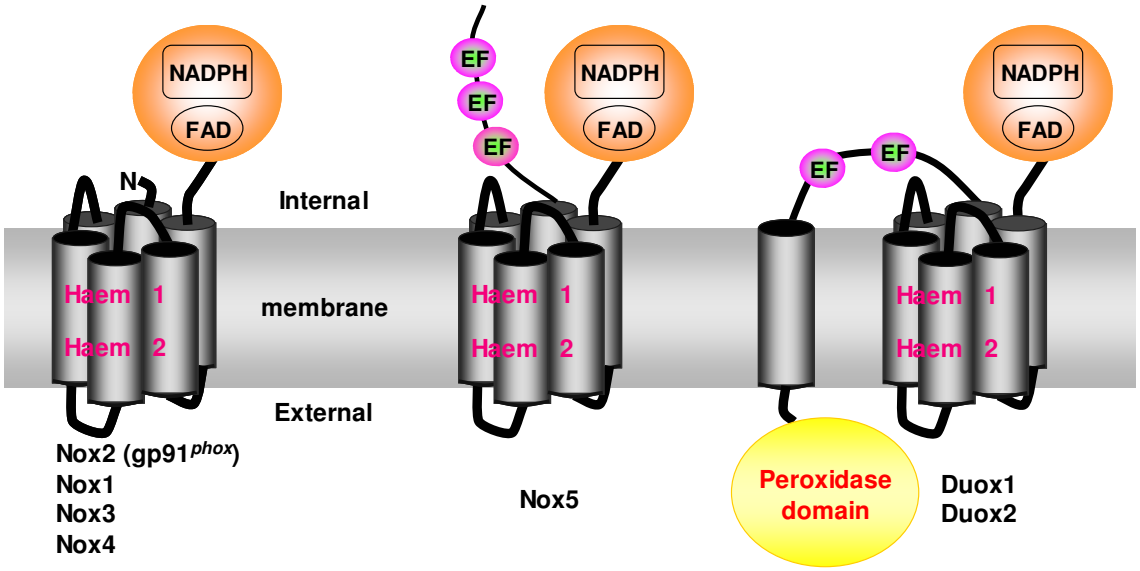

Figure 10. Transmembrane topology and structural domains of Nox/Duox enzymes. Structural motifs in Nox/Duox family are present as indicated. Transmembrane domains are shown in shaded cylinders, containing one pair of haems. In Nox/Duox family, the C-terminal region contains the NADPH- and FAD-binding sites. An additional transmembrane domain is present in Duox1/2 followed by an extended N-terminal domain homologous to peroxidase. EF hand motifs are present in Nox5 and Duox1/2.

Consistent with their Ca^{2+}-binding EF hand domains, Nox5 and Duox1/2 are Ca^{2+}-activated enzymes (Banfi et al. 2000; Banfi et al. 2001).

Nox1 was initially cloned from a colon epithelial cell cDNA library and referred to as Mox 1 (*M*itogenic *ox*idase 1) for its mitogenic regulation in transfected 3T3 cells (Suh et al. 1999). Banfi *et al.* cloned the same gene based on a sequence associated with H^+ channels, and named it as NOH-1 (NADPH oxidase homologue-1) (Banfi et al. 2000). Nox1, abundantly expressed in the colon, generates low amounts of ROS. It is believed to play a role in the host defence through ROS-dependent bacterial killing in colon (Lambeth 2002). Nox3 is highly expressed in the inner ear. Nox3-transfected HEK293 cells generated low levels of ROS, suggesting that Nox3 is a superoxide-producing enzyme (Banfi et al. 2004). In the Nox3-deficient mouse, lack of otoconia formation and subsequent troubles of equilibrium were observed (Paffenholz et al. 2004). This suggests that Nox3 maybe play a role in the biosynthesis of otoconia. Nox4 was originally referred to as Renox (*Ren*al *ox*idase) for its abundant expression in the kidney cortex. It is suggested to play a role in the oxygen sensing

Table 2 Human Nox/Duox family of NADPH oxidase (Cheng et al. 2001; Vignais 2002; Cross et al. 2004)

Isoform (synonyms)	Locus	Amino acids	Sequence similarity to Nox2	Tissue distribution	Known regulatory factors	Possible function
Nox1 (MOX1, NOH1)	Xq22	564	53%	Colon, vascular smooth muscle	NoxO1, NoxA1 and $p22^{phox}$	Mitogenic signaling, proton channel, Host defense
Nox2 ($gp91^{phox}$)	Xp21,1	570		Phagocytes, lymphocytes, dendritic cells	$p47^{phox}$, $p67^{phox}$, $p40^{phox}$, $p22^{phox}$ and Rac1/Rac2	Host defense
Nox3	6q25.1-q26	568	58%	Fetal kidney, Inner ear	N.D.	?
Nox4 (Renox)	11q14.2-q21	578	37%	Kidney, osteoclasts, ovary and eye; widespread	N.D.	Oxygen sensing /signaling
Nox5	15q22	747	27%	Spleen, sperm, mammary glands and cerebrum	Calcium	?
Duox1 (p138Tox)	15q21	1551	29%	Thyroid, cerebellum and lung	Calcium	Thyroxin synthesis /extracellular matrix
Duox2	15q21	1548	29%	Thyroid, colon, pancreatic islets and prostate	Calcium	Extracellular matrix

in this tissue (Geiszt et al. 2000). Nox4 is also expressed in placenta and glioblastoma cells (Cheng et al. 2001). Nox4-transfected HEK293 cells generated low levels of superoxide, and this superoxide-generation could significantly been increased by co-expression with $p22^{phox}$ (Ambasta et al. 2004).

Nox5 is found in lymphoid tissues and testis. It mediates Ca^{2+}-dependent ROS generation in these tissues (Banfi et al. 2001). Duox1/2 are both expressed in thyroid and therefore referred to as Thox (*Ty*roid *ox*idase) (De Deken et al. 2000). Duox1/2 are believed to be involved in the synthesis of thyroid hormones. In general, these homologues of Nox2 are expressed in epithelial cells and would be expected to transfer electron across membranes to oxygen (Cross et al. 2004). Low levels of ROS produced by Nox2 homologues in non-phagocytic cells could have a role in host defence (Banfi et al. 2001), signal transduction (Suh et al. 1999), and oxygen sensing (Geiszt et al. 2000; Lambeth 2002). However, their exact physiologic role and their regulation are not fully understood.

There is cross-talking between Nox1 and the cytosolic factors of Nox2: Nox1 can been activated when it is co-expressed with NoxO1 and $p67^{phox}$, or with NoxA1 and $p47^{phox}$ (Banfi et al. 2003; Geiszt et al. 2003*a*; Takeya et al. 2003). The Nox1/3/4-dependent superoxide generation requires the co-expression of $p22^{phox}$, supporting the involvement of $p22^{phox}$ in Nox system (Ambasta et al. 2004). These informations suggest that the same motif in Nox family could play a similar role in the superoxide-generation process.

Nox-2S

More recently, a novel isoform of Nox2 was identified as Nox-2S (Heidari et al. 2004). Nox-2S is a splice variant of Nox2 and includes an unidentified exon, mapped 6.4 kb downstream of exon 3. It comprises 114 amino acids with a molecular mass of 14.7 kDa. Nox-2S displays a widespread pattern of mRNA expression in mouse tissues and human cells, with high levels present in the myeloid cell line HL-60. The function of Nox-2S awaits elucidation.

4. Activation and assembly of NADPH oxidase

Phagocytes can be activated by a variety of physiological stimuli through binding to seven-transmembrane cell-surface receptors associated with G-protein. G-protein subsequently dissociates into different subunits (α and β/γ subunits) which interact with three phospholipases, PLC, PLD, and PLA_2. The source of lipids used by these lipases is from the phagocyte's plasma membrane (Thrasher et al. 1994) (Figure 11). These stimuli include C5α (complement fragment 5α), fMLP (N-formyl methionyl-leucyl-phenylalanine), PAF (platelet-activating factor), LTB4 (leukotriene B4) and IL-8. The α and β/γ subunits of the G protein produced during activation, activate phospholipase C (PLC), which hydrolyses the lipid precursor PIP_2 (phosphatidylinositol 4,5-biphosphate) to produce IP_3 (1,2,5-triphosphate) and DAG (diacylglycerol). DAG may be also generated by PA (phosphatidic acid), the product of phospholipase D (PLD). Arachidonic acid is derived from glycurophospholipids by PLA_2 activity. These lipid messengers act on various cellular targets as second messengers (Figure 11). IP_3 releases Ca^{2+} from intracellular pools, and DAG in the presence of Ca^{2+} activates several isoforms of PKC which phosphorylate proteins such as $p47^{phox}$ and $p67^{phox}$.

Ca^{2+} may also activate Ca^{2+}-dependent PKs leading the actin cytoskeleton regulation. PA can either directly activate various kinases and phosphatases or be hydrolyzed by PA phosphohydrolase to produce DAG. In addition, arachidonic acid could activate several kinases.

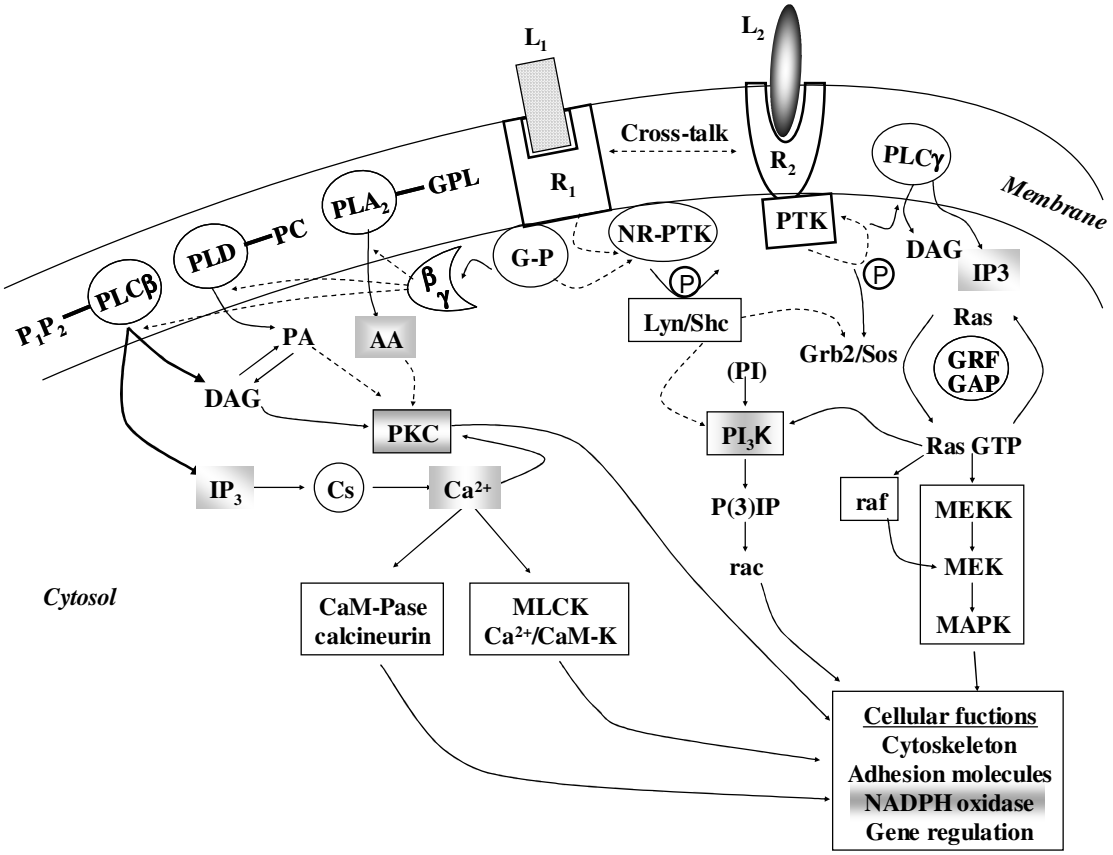

Figure 11. Schematic presentation of the main transductional pathways in phagocytes (Labro 2000). The main abbreviations are given in the text. Additional abbreviations: R1 and R2 receptors; L1 and L2 ligands; Cs, calciosome; CaM-K/CaM-Pase, calmodulin-dependent kinase/phosphatase; GAP, GTPase-activating protein; GRF, guanine regulatory exchange factor; GP, heterotrimeric G protein; GPL, glycurophospholipids; MLCK, myosin light-chain kinase; NR-PTK/PTK, nonreceptor/receptor protein tyrosine kinase; P, phosphorylation; PC, phosphatidylcholine.

Chemoattractant signaling also involves G-protein-coupled activation of various tyrosine kinases of the Src family (Figure 11), including the tyrosine kinase Lyn, which phosphorylates various adapter proteins such as Shc. The Shc-P-Lyn complex may activate phosphatidylinositol 3-kinase (PI_3-K), catalyzing the addition of a phosphate group to the D3-position of phosphatidylinositol lipids. Grb2, linked to ShC, is generally associated with Sos (the Ras guanine nucleotide exchange regulator) and mediates the activation of the monomeric G protein Ras, activating the mitogen-activated protein (MAP) kinase cascade and Raf serine/threonine kinase, which could activate the kinase MEK (MAP kinase kinase) (Labro 2000). All these second messengers and associated signaling pathways are reponsable for the activation of NADPH oxidase.

PMA (phorbol 12-myristate 13-actetate), mimicking the effects of DAG, can directly activate some intracellular protein kinase C isoforms (PKCs). Ionomycin, a Ca^{2+} ionophore, activates NADPH oxidase by increasing free Ca^{2+} by its ionophore activity.

4.1 NADPH oxidase assembly during activation

4.1.1 *Interaction between cytosolic components*

In the resting state, $p67^{phox}$ is the bridge to connect $p40^{phox}$ and $p47^{phox}$ in cytosol of neutrophils (Lapouge et al. 2002). Crystal structure analysis tryptophan fluorescence study demonstrated that SH3 domain of $p40^{phox}$ can interact with a consensus polyproline motif (residues 360-369) of $p47^{phox}$ C-terminus (Massenet et al. 2005) (Figure 4). Residues 360-369 of $p47^{phox}$ interact with SH3 domain of $p40^{phox}$ mainly via van der waals contacts involving Phe^{179}, Asn^{184}, Asp^{206}, Trp^{207}, Pro^{220}, and Phe^{223} of $p40^{phox}$.

Upon activation, phosphorylation induces a conformational change in $p47^{phox}$, leading to several protein-protein interactions (Figure 12). Its PRR domain interacts with the C-terminal

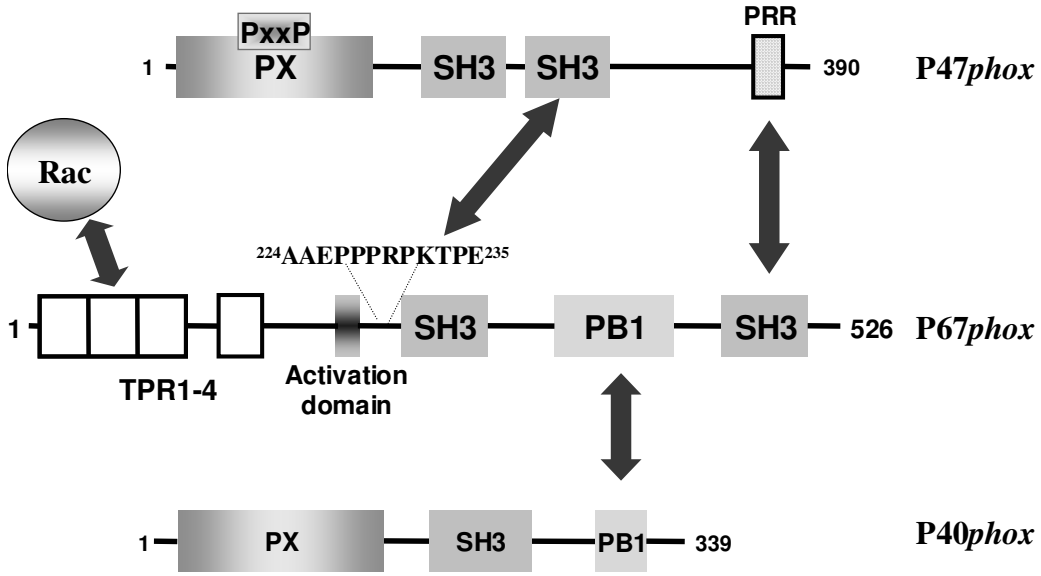

Figure 12. Interaction of cytosolic components during the NADPH oxidase activation. The sites of protein-protein interaction are indicated by arrows.

SH3 domain of $p67^{phox}$ (Leto et al. 1994; Deleo et al. 1996). This interaction is suggested to occur independently of the remainder of both proteins (Lapouge et al. 2002). The C-terminal SH3 domain of $p47^{phox}$ could interact with a proline rich region (residues 224-235) in the N-terminal of $p67^{phox}$ (Leto et al. 1994; De Mendez et al. 1996; Massenet et al. 2005). During oxidase activation, Rac switches to its active GTP-bound form, and interacts with the TRP region of $p67^{phox}$ by multiple hydrogen bonds (Figure 12). The binding of Rac to $p67^{phox}$ is essential for the oxidase activation (Diekmann et al. 1994). Crystallographic data indicated that Arg^{102} in $p67^{phox}$ plays a key role in Rac-$p67^{phox}$ complex formation through hydrogen-binding with several residues of Rac (Lapouge et al. 2000).

Interestingly, most of A67-CGD mutations are located in the N-terminal region of $p67^{phox}$. The investigation of two A67-CGD mutations (Gly78Glu and Ala128Val) indicated that Gly78Glu mutant leads to a misfolding of the protein by steric hindrance within the TPR3 motif, whereas Ala128Val has less drastic effect on the structure, presenting the capability to

bind Rac and to activate the NADPH oxidase in a CFS assay (Grizot et al. 2001*a*). Mutant forms of Rac (Diekmann et al. 1994) and a series of TPR mutants of $p67^{phox}$ (Koga et al. 1999) in which the interaction between $p67^{phox}$ and Rac was destroyed were unable to activate the NADPH oxidase *in vitro*. This suggests that $p67^{phox}$ in association with Rac may be an essential factor for activating the electron transfer within cytochrome b_{558} (Vignais 2002). $P40^{phox}$ interacts with PB1 domain of $p67^{phox}$ by its PB1 domain. In addition, the small-angle neutron scattering analysis suggested that the role of amphiphiles (SDS or arachidonic acid) or phosphorylation of $p47^{phox}$ in the activation of NADPH oxidase could disrupt the $p47^{phox}$-$p40^{phox}$ complex rather than to break an intramolecular interaction in $p47^{phox}$ (Grizot et al. 2001*b*).

4.1.2 *Interaction between cytosolic factors and cytochrome b_{558}*

▸ p47*phox* with cytochrome b_{558}

$P47^{phox}$ is believed to play a central role in the NADPH oxidase assembly process. $P67^{phox}$ failed to translocate to the membrane-bound cytochrome b_{558} in the $p47^{phox}$-deficient CGD. However, the translocation of $p47^{phox}$ is not impaired in $p67^{phox}$-deficient CGD (Heyworth et al. 1991). It is consistent with the report that $p47^{phox}$ precedes $p67^{phox}$ in the active oxidase complex formation by its association with cytochrome b_{558} (Kleinberg et al. 1990). The conformational changes of $p47^{phox}$ induced by extensively phosphorylation, expose the unmasked SH3 to interact with the PRR region (residues 149-162) of $p22^{phox}$ (Figure 12).

Identification of essential oxidase components and their binding interactions have resulted from studies using a CFS assay, developed by Heyneman and Vercauteren (Heyneman et al. 1984) and Bromberg and Pick (Bromberg et al. 1985). This system is composed of neutrophil plasma membranes or purified cytochrome b_{558} and neutrophil cytosol or recombinant proteins, $p47^{phox}$, $p67^{phox}$, and Rac (Abo et al. 1992). The system is activated *in vitro* by GTPγS and an amphiphilic agent (SDS or arachidonic acid) in the presence of NADPH. However, the oxidase activation in a CFS assay occurs in a non-physiological environment, e.g. phosphorylation of $p47^{phox}$ is not required in this system. A synthetic peptide corresponding to residues 175-194 of $p22^{phox}$ inhibits the NADPH-dependent oxygen uptake *in vitro* and interacts with $p47^{phox}$, demonstrating that the C-terminal of $p22^{phox}$ is a binding site for $p47^{phox}$ (Nakanishi et al. 1992).

A human missense mutation (Pro156Gln) in a $A22^{+}$-CGD, located in the PRR region of $p22^{phox}$ leads to a defective translocation of $p47^{phox}$ (Leusen et al. 1994*b*) (Figure 3). Arachidonic acid and SDS, the *in vitro* activators of the oxidase, cause the exposure of SH3 domains of $p47^{phox}$, which can bind to $p22^{phox}$, but not to its mutant Pro156Gln-$p22^{phox}$ (Sumimoto et al. 1994). Deletion analysis of $p47^{phox}$ in transfected K562 cells demonstrated multiple SH3-mediated interactions between $p47^{phox}$ and cytochrome b_{558} (De Mendez et al. 1996).

Based on the random-sequence peptide phage display library analysis, two domains (^{156}PPRPP^{160} and ^{177}GGPPGGP^{183}) located within proline-rich region of $p22^{phox}$ were proposed to represent putative binding motifs for $p47^{phox}$ (DeLeo et al. 1995*a*) (Figure 3). By the same approach, residues 322-342 of $p47^{phox}$ has been indicated to associate with cytochrome b_{558} (DeLeo et al. 1995*b*) (Figure 4). The substitution Trp193Arg in the N-terminal SH3 domain of $p47^{phox}$ completely abrogates its association with $p22^{phox}$ and this

mutant protein is incapable to support superoxide production in a CFS assay. This suggests that the interaction between the N-terminal SH3 domain of p47^{phox} and the PRR domain of p22^{phox} is essential for the oxidase activation (Sumimoto et al. 1996). "Peptide walking" analysis demonstrated that p22^{phox} is an anchor for p47^{phox} and that p22^{phox} interacts with p47^{phox} by its PRR (Dahan et al. 2002).

P47^{phox} has also been proposed to interact with gp91^{phox} during the oxidase activation. A synthetic peptide corresponding to residues ^{559}RGVHFIF^{565} of the C-terminus of gp91^{phox} inhibited NADPH oxidase activation when allowed to diffuse into electrically permeabilized neutrophils before stimulation with fMLP or PMA (Rotrosen et al. 1990) (Figure 3). The authors concluded that this special region in gp91^{phox} may mediate interaction with cytosolic factors. Based on the study of the substitution of Arg, Val, ILeu and Phe within this region by Ala, Kleinberg *et al.* found similar results (Kleinberg et al. 1992). Other groups demonstrated that this peptide inhibits superoxide generation and p47^{phox} membrane-translocation *in vitro* (Park et al. 1997; Tsuchiya et al. 1999). Another synthetic peptide corresponding to residues 550-569 inhibits oxidase activity induced by SDS in CFS assay and can interact with p47^{phox}, indicating that this C-terminal region of gp91^{phox} is the binding site for p47^{phox} (Nakanishi et al. 1992). However, based on the kinetic inhibitory study induced by the ^{559}RGVHFIF^{565} peptide, Uhlinger *et al.* suggested that this peptide may bind to and alter the conformation of cytochrome b_{558}, rather than competing for cytochrome b_{558}-p47^{phox} interactions (Uhlinger et al. 1995). However, by mutagenesis approach, the distal C-terminus of gp91^{phox} was found to be determinant for the gp91^{phox} stability, but neither the ^{559}RGVHFIF^{565} sequence nor a carboxyl-terminal aromatic residue (Phe^{570}) were absolutely required for NADPH oxidase activity in intact granulocytic cells (Zhen et al. 1998).

The missense mutation Asp500Gly in gp91^{phox} responsible for an X^{+}-CGD, led to a defective p47^{phox} and p67^{phox} translocation to the plasma membrane in the patient neutrophils. In addition the synthetic peptide residues 491-504 inhibited NADPH oxidase activity in a CFS assay (Leusen et al. 1994*a*). However, in another X^{+}-CGD study (deletion of residues 488–497 in gp91^{phox}), the *in vivo* and *in vitro* translocation of p47^{phox} and p67^{phox} to Δ488-497 gp91^{phox} PLB-985 plasma membranes was not affected, and the synthetic peptide corresponding to residues 488-497 was ineffective to inhibit superoxide generation in a CFS assay (Yu et al. 1999*b*). On the contrary, mutagenesis study of this region suggested that residues 484-500 of gp91^{phox} are crucial for NADPH oxidase activation and oxidase assembly process (Li et al. 2005).

Two other gp91^{phox}-p47^{phox} interaction sites have been identified by phage display. They encompass residues ^{87}STRVRRQL^{93} and ^{451}FEWFADLL^{458} of gp91^{phox} (DeLeo et al. 1995*b*). Mutagenesis of residues 86-102 (the intra-cytosolic B-loop of gp91^{phox} seen in Figure 7 demonstrated that Arg^{91} and Arg^{92} of gp91^{phox} are essential for cytochrome b_{558} function in granulocytes. Defective p47^{phox} and p67^{phox} translocation to the plasma membranes from R91E/R92E gp91^{phox} mutant transfected PLB-985 cells, suggests that these arginines play a central role in the oxidase assembly (Biberstine-Kinkade et al. 1999).

▸ P67*phox* with cytochrome b_{558}

The interaction of p47^{phox} with cytochrome b_{558} is well established, however those between p67^{phox} and cytochrome b_{558} has been less investigated. "Peptide walking" approach

revealed that p67^{phox} can bind to residues 151-160 (PRR) of p47^{phox} and to two additional domains containing residues 81-91 and 111-115 of p22^{phox} (Dahan et al. 2002). The group of Babior found a direct interaction between p67^{phox} and cytochrome b_{558} by several experiments. Labeled p67^{phox} recognized a 91-kDa band in specific granules from a normal patient but not from a cytochrome b_{558} deficient patient; P67^{phox} was able to bind to pure cytochrome b_{558} that had been applied to nitrocellulose. Cytochrome b_{558} could be affinity-precipitated by GST-p67^{phox} (glutathione S-transferase) coupled to glutathione-Sepharose beads (Dang et al. 2001).

The N-terminal region of p67^{phox} has a higher binding affinity to cytochrome b_{558} than the full-length p67^{phox}, suggesting that this N-terminal domain of p67^{phox} serves as binding site for cytochrome b_{558}. This N-terminus is probably masked partially by the C-terminus of p67^{phox} in the full-length p67^{phox} (Dang et al. 2002). This hypothesis was supported by the results that the C-terminal residues 211-526 of p67^{phox} were not needed for cell-free oxidase activity. The importance of the N-terminal domain of p67^{phox} is also shown by the fact that the mutation Val204Ala (located in the activation domain) is totally inactive (Han et al. 1998) (Figure 4). In the study of a series of truncated forms of gp91^{phox}, Nisimoto *et al.* demonstrated that C-terminus of gp91^{phox} (221-570 residues) displayed the diaphorase activity in the presence of the N-terminus of p67^{phox} (1-210 residues) (Figure 5, 7).

Rac is absolutely required for the activity in this CFS assay, confirming that N-terminus of p67^{phox} and Rac are minimal essential effectors for the activation (Nisimoto et al. 2004). Koga *et al.* found that the first three TPR domains of p67^{phox} interact with Rac (Figure 5). The substitution Arg102Glu completely abrogated the capability of activating the oxidase, suggesting that Arg^{102} in the third TPR domain is likely involved in binding to Rac (Koga et al. 1999). Based on the study of the binding of [^{32}P]NADPH dialdehyde to p67^{phox}, Smith *et al.* concluded that p67^{phox} contains a catalytic NADPH-binding site which is located in its N-terminus (Figure 5)(Smith et al. 1996).

4.2 Interaction between oxidase cytosolic components and membrane lipids

It appears that p47^{phox} and/or p67^{phox} translocation to membrane-bound cytochrome b_{558} depends on the interaction with both p22^{phox} and gp91^{phox}. P47^{phox} drives assembly, triggering the translocation and the interaction between different oxidase components through discrete domains. The interactions between the cytosolic components of oxidase and membrane-lipids are required for membrane translocation of p47^{phox} and p40^{phox} (Kanai et al. 2001; Zhan et al. 2002; Stahelin et al. 2003). P47^{phox} and p40^{phox} contain PX domain which has recently been reported to bind to phosphoinositides. Upon activation, the N-terminal unmasked PX domain of p47^{phox} (residues 4–128) (Figure 12) has been demonstrated to bind to specific membrane phosphoinositides and may thus mediate in part the oxidase assembly (Kanai et al. 2001; Stahelin et al. 2003). X-ray crystal structures of the PX domain has revealed the basis of stereospecific recognition of PtdIns(3,4)P_2 for p47^{phox}. The Arg42Gln mutation in this domain abolished its phosphoinositide binding, supporting that the PX domain of p47^{phox} is indispensable for its membrane lipid-binding (Kanai et al. 2001).

Although the role of p40^{phox} in the oxidase activation is controversial (positive or negative regulator), this cytosolic component could bind to PtdIns(3)P by its PX-domain (Stahelin et al. 2003; Zhan et al. 2002). The membrane recruitment of p47^{phox} and p40^{phox} by

their PX domain is under control of phosphatidylinositol 3-kinase (PI3) activity (Zhan et al. 2002). However, it was recently shown that phosphoinositide interaction is required, but likely not sufficient, for membrane translocation of $p47^{phox}$ (Ago et al. 2003). A recent proteomic study identified that the presence of lipid rafts in neutrophils, including cytoskeletal proteins and several membrane proteins such as Fc receptor proteins (Nebl et al. 2002). This confirms the general conception that these lipid compartments function as physical platforms for signal integration at the plasma membrane. Segal and collegues found that the components of NADPH oxidase are localized in these lipid microdomains. Indeed lipid rafts mediate the efficiency of oxidase coupling to receptors (Shao et al. 2003).

Upon activation, Rac is recruited to the plasma membrane associated with the insertion of the geranylgeranyl tail into the phospholipids bilayer (Vignais 2002). Rac1 was found to be the least impaired factor in membrane translocation after cholesterol depletion, suggesting that Rac translocates to the membrane by a mechanism independent of lipid rafts (Vilhardt et al. 2004). Finally Vilhardt and van Deurs proposed that assembly of the NADPH oxidase complex depends on multiple weak, but cooperative binding interactions, presumably greatly favored in a raft environment (Vilhardt et al. 2004).

The membrane-translocation of $p47^{phox}$ and $p67^{phox}$ required the presence of cytochrome b_{558}, while Rac membrane-translocation is independent of $p47^{phox}$ and $p67^{phox}$ (Heyworth et al. 1994).

5. Chronic granulomatous disease (CGD)

Chronic granulomatous disease (CGD) is a rare congenital disorder in which phagocytic cells (neutrophils, eosinophils, monocytes and macrophages) fail to generate superoxide (O_2^-) and is characterized by severe recurrent bacterial and fungal infections after ingesting them (Johnston et al. 1977). This disease is characterized by a greatly increased susceptibility to severe recurrent bacterial and fungal infections that are difficult to treat by conventional means. CGD is a rare primary immunodeficiency, with an estimated incidence of 1 in about 250,000 individuals, without ethnic preference. Patients usually present clinical syndrome in the first few years of life with cervical or inguinal lymphadenitis, liver abscesses, osteomyelitis, pneumonia or skin infections (Segal 1996). Although a board range of bacteria, including *Pseudomonas cepacia*, the commonest pathogen is *Staphylococcu aureus*.

The investigation of the molecular basis of CGD was demonstrated to elucidate the mechanisms responsible for the respiratory burst. The identification of most oxidase components ($gp91^{phox}$, $p67^{phox}$ and $p47^{phox}$) was determined through their absence from the cells of CGD patients (Royer-Pokora et al. 1986; Volpp et al. 1988; Nunoi et al. 1988). CGD is a very heterogenous disorder causing by mutations in any one of four subunits of NADPH oxidase (Thrasher et al. 1994; Segal 1996; Heyworth et al. 2003) (Table 3). In table 3, the superscript denotes the level of protein: undetectable (^{0}), diminished ($^-$) or normal ($^+$), as determined by immunoblot analysis and/or spectral analysis (Heyworth et al. 2001). The most common form of CGD is due to X-linked recessive defect in $gp91^{phox}$, which accounts for about 60% of cases, exclusively in males. The other three forms of this disease are due to an autosomal recessive transmission due to defect in other components of the oxidase, $p22^{phox}$, $p47^{phox}$ or $p67^{phox}$, causing about 5%, 30% and 5% of cases, respectively.

Table 3 Classification of CGD

Component	Nox2 (gp91*phox*)	p22*phox*	p47*phox*	p67*phox*
Disease	X-linked	Autosomal recessive	Autosomal recessive	Autosomal recessive
	$X91^0$ CGD (55%)	$A22^0$ CGD (5%)	$A47^0$ CGD (30%)	$A67^0$ CGD (5%)
	$X91^-$ CGD (<5%)			$A67^-$ CGD (1 case)
	$X91^+$ CGD (<5%)	$A22^+$ CGD (1 case)		

5.1 Autosomal CGD (A-CGD)

A47-CGD

Mutations in *NCF-1* gene encoding $p47^{phox}$ cause the most common autosomal CGD form, the $A47^0$ CGD, accounting for about 30% of all CGD cases. In contrast to the other types of CGD, in which a high heterogeneity exists among mutations, a unique mutation has been identified in approximatively 94% of affected alleles from $A47^0$ CGD patients (Cross et al. 2000). This mutation is a dinucleotide deletion of GT from a GTGT tandem in the first four nucleotides of exon 2, causing a frameshift which results in a premature stop codon (Casimir et al. 1991, Cathebras et al 2001). The predominance of this mutation arises from the possible recombination events between *NCF-1* and its highly homologous pseudogenes (*ΨNCF-1*) (Roelser et al. 2000; Vazquez et al. 2001).

A67-CGD

The A67-CGD represents a rare subtype of CGD, accounting approximetely for 5% of CGD cases. In the 24 A67-CGD patients, 34 different mutations have been found among 48 alleles (Cross et al 2000; Roos et al. 2003). Most of A67-CGD patients had no expression of $p67^{phox}$ protein with normal levels of mRNA (Roos et al. 2003). Interestingly, an A67-CGD mutation (a T-to-C transition in the conservative 5' splice site of the intron 3) resulted to a deletion in mRNA from 174 bp to 258 bp, leading to a drastically diminished mRNA expression. In addition this mutation generated a premature TGA stop codon at position 60, resulting to the absencce of $p67^{phox}$ in the patient (Tanugi-Cholley et al. 1995). Only one case ($A67^-$-CGD) expressing half-normal amount of one amino acid-deleted (Lys^{58}) $p67^{phox}$ has been reported (Leusen et al. 1996) (Figure 5). This mutation in $p67^{phox}$ disturbs its interaction of Rac. Both $p47^{phox}$ and $p67^{phox}$ did not translocate to the patient's plasma membrane upon cell activation, indicating that an interaction between $p67^{phox}$ and Rac is essential for the assembly process. It is not in agreement with that observed in an $A67^0$-CGD in which the translocation of $p47^{phox}$ occurred normally (Heyworth et al. 1991).

A22-CGD

Defects in the *CYBA* gene encoding $p22^{phox}$, the light chain of cytochrome b_{558} also lead to a rare CGD variant. Mutations are variables including deletions, insertions, splice site mutations nonsense and missense mutations (Stasia et al. 2002*b*, Cross et al 2000). The only $A22^{+}$ mutation is caused by a substitution Pro156Gln (Dinauer et al. 1991), located in the PRR region of $p22^{phox}$ that serves as a binding site for the N-terminal SH3 domain of $p47^{phox}$ (Figure 3). Independently, three groups have shown, in the CFS assay (Sumimoto et al. 1994) as well as in transfected cells (Leto et al. 1994) and in patient's neutrophils (Leusen et al. 1994*b*), that this mutation abolished the association of $p47^{phox}$ with $p22^{phox}$. These data suggest that the translocation of $p47^{phox}$ and $p67^{phox}$ to cytochrome b_{558} needed for the oxidase activation, depends on interactions with both $p22^{phox}$ and $gp91^{phox}$.

5.2 X-CGD

Only four polymorphisms in the *CYBB* gene have been reported (Kuribayashi et al. 1996; Jirapongsananuruk et al. 2002; Heyworth et al. 2001) (Table 4). Mutations (deletions,

Table 4 Known polymorphisms in the *CYBB* gene (Heyworth et al. 2003)

Nucleotide change	Effect	Approximately frequency (%)
G1014A	Silent (Lys334)	1
G1102C	Gly364Arg	1
T1563A	Asp517Glu	1
3' intron 5 gcag/acag	Slice	1

insertions, splice site mutations, missense mutations and nonsense mutations) in the *CYBB* gene usually lead to lack of $gp91^{phox}$ protein expression, due to instability of mRNA and /or protein. This type of X-linked CGD is referred as X^0 CGD, characterized by an absent cytochrome b_{558} in the patient neutrophils (Royer-Pokora et al. 1986; Roos et al. 1996*a*). This subtype accounts for most of X-CGD cases (Table 3).

A few rare cases of mutations in the *CYBB* resulting in low expression of cytochrome b_{558} have been identified as X^- CGD (Table 3). In some cases, X^- CGD results in weak oxidase activity associated with low levels of cytochrome b_{558} expression detected in the entire population of neutrophils (Roos et al. 1996*a*; Stasia et al. 2003). However, the clinical severity is not always related to the superoxide production led by the patients' neutrophils (Stasia et al. 2003). Only four different mutations in the promoter region around -55 bp of *CYBB* gene led to an X^- CGD type.

Very few rare mutations have been found to yield normal expression of $gp91^{phox}$ with a defective oxidase activity. This subtype of CGD is called X^+-CGD. This rare variant is of

interest because relationship between the structure and the function of gp91^{phox} can be established by this way. 16 X^+-CGD mutations (Table 6) have contributed to elucidate functional domains of gp91^{phox} in the oxidase activation process (Heyworth et al. 2003).

▸ X^--CGD

26 mutations have been found in X^--CGD patients (Heyworth e al. 2001; Stasia et al. 2005) (Table 5). These variants are of interest because they result from structural disorganization, leading to an incomplete loss of protein, partial dysfunction, or both (Stasia et al. 2003). Four X^--CGD mutation are located in the promoter region of the *CYBB* gene, two of them resulted from mutations A-57C and T-55C (case 1 and 2, Table 5). A small subset (5% to 10%) of neutrophils expressed near normal levels of cytochrome b_{558} and oxidase activity, while the remaining cells completely lacked both in these variant cases (Newburger et al. 1994; Woodman et al. 1995). However, Stasia and collegues (Stasia et al. 2003) found that for the same mutation (T-55C) the neutrophils' population had a diminished but homogeneous gp91^{phox} expression with a measurable level of NADPH oxidase activity (3-9% of normal). Despite the low level of gp91^{phox} expression and the residual NADPH oxidase activity in patients' phagocytes, the clinical appearance was severe.

The other two mutations in the promoter (C-53T and C-52T) were reported to lead X^--CGD (cases 3 and 4, Table5). All these promoter mutations are located in a region between the "CCAAT" and the "TATA" boxes in a consensus binding for the *ets* family of transcription factors of gp91^{phox} promoter site (5'-GAGGAAAT-3', lower strand, -57 to -50 bp). A-57C, T-55C, and C-53T mutations strongly inhibit the binding of both Elf-1 and PU.1 (members of *ets* family of transcription factors abundantly expressed in myeloid cells), suggesting that these mutations reduce gp91^{phox} promoter activity, resulting to a low level of gp91^{phox} expression (Stasia et al. 2003).

Most of X^--CGD mutations are located in a functional domain of gp91^{phox} (Table 5). Four deletion mutations and only one splice site mutation lead to X^--CGD, but most of X^--CGD resulted from missense mutations. Two mutations (His101Tyr and His209Tyr) are located in the haem-binding sites of gp91^{phox} (Figure 7) (Bolscher et al. 1991; Tsuda et al. 1998). The mutation His101Tyr totally inhibits superoxide generation in patient neutrophils,in which a small amount (about 10% of control) of cytochrome b_{558} was detected (Tsuda et al. 1998). These data suggest that the haem incorporation to gp91^{phox} is required for the expression of the large subunit of cytochrome b_{558}. The X^--CGD mutations (Ala157, Lys161Arg and Cys244) are located at the second and third extra-loops, which contain the Asn residues as glycosylated sites (Figure 7). These mutations could affect the glycosylation of gp91^{phox}, leading to an unstable mutated gp91^{phox}. Ser193Phe (Roesler et al. 1999) mutation is located in the second intracellular loop of gp91^{phox}, which is an important domain in the Nox family (Li et al. 2005). The molecular mechanism of this X^--CGD mutation is under investigated in our laboratory.

Interestingly, two neighboring missense mutations (His338Tyr and Pro339His) (Roos et al. 1996*a*; Yoshida et al. 1998; Ariga et al. 1994; Roos et al. 1996*b*) are located in the putative binding site for the isoalloxazing ring of FAD moiety (^{338}HPFT^{341} motif), which is heavily conserved in FNR family. His338Tyr mutation disturbed superoxide production in patient

neutrophils, which contained a diminished expression of gp91^{phox} with one-third levels of the haem by contrast to normal control. The translocation of p47^{phox} and p67^{phox} occurred

Table 5 Mutations in *CYBB* gene for gp91*phox* that cause X^{-}-CGD (Heyworth 2003)

Case	cDNA nucleotide (or splice site) change	Mutation	Amino acid change	Potential structral / functional domain	Functional analysis	Reference
1	A-57C	Promoter	NA			Newburger et al. 1994
2	T-55C	Promoter	NA			Newburger et al. 1994; Stasia et al. 2003
3	C-53T	Promoter	NA			Kuribayashi et al. 1995; Roos et al. 1996
4	C-52T	Promoter	NA			Suzuki et al. 1998
5	G66C	Missense	Trp18Cys	I-transmembrane helix		Roos et al. 1996b
6	C170A	Missense	Ala53Asp	II-transmembrane helix (near the haem-binding site)		Roos et al. 1996a
7	C179T	Missense	Pro56Leu	II-transmembrane helix (near the haem-binding site)		Roos et al. 1994; Winkelstein et al. 2000
8	G188T	Missense	Cys59Phe	II-transmembrane helix (near the haem-binding site)		TSRI
9	C311T	Missense	His101Tyr	Haem-binding	His101 is one of the haem-binding ligands	Tsuda et al. 1998
10	G478A	Missense	Ala156Thr	II-extra loop (near the glycosylation site)		Bolscher et al. 1991; Curnutte et al. 1995
11	A494G	Missense	Lys161Arg	II-extra loop (near the glycosylation site)		Curnutte et al. 1995
12	571-579 ATATTAATT deletion	Deletion	187-189 IleLeulle deletion	IV-transmembrane helix		TSRI
13	C590T	Missense	Ser193Phe	II-intra loop (D-loop)		Roesle et al. 1999
14	C637T	Missense	His209Tyr	Haem-binding		Bolscher et al. 1991
15	G743C	Missense	Cys244Ser	III-extra loop (near the glycosylation site)		Bolscher et al. 1991; Winkelstein et al. 2000
16	G743A	Missense	Cys244Tyr	III-extra loop (near the glycosylation site)		Bu-Ghanim et al. 1995
17	G937A	Missense	Glu309Lys			Segal et al. 2000
18	948/957 GAA (or AAG)	Deletion	313, 314 or 315 Lys			Segal et al. 2000; Bu-Ghanim et al. 1995
19	G977A	Missense	Gly322Glu			Rae et al. 1998
20	A985T	Missense	Ile325Phe			Rae et al. 1998
21	C1024A	Missense	His338Tyr	The isoalloxazing ring of FAD moiety bindingsite	His338 is very critical for FAD incorpration	Roos et al. 1996*a*; Yoshida et al. 1998
22	C1028A	Missense	Pro339His	The isoalloxazing ring of FAD moiety bindingsite		Ariga et al. 1994; Roos et al. 1996*b*
23	3' intron 9 t(8nt)ag/g(8nt)ag	Splice site	Deletion exon 10/normal mRNA			Roesler et al. 1999
24	G1178C	Missense	Gly389Ala			Bolscher et al. 1991
25	11 bp deletion: 2 bp of the end of exon 12 + 9 bp of the beginning of intron 12	Deletion	Frameshift at 524 and introduction of a stop codon at 534	Lost the nicotinamide-binding site (^{535}FLCGPE^{540})		Stasia et al. 2005
26	1612-1626 deletion	Deletion	AA 534-538 deletion	Lost the nicotinamide-binding site (^{535}FLCGPE^{540})		TSRI

normally. However, the FAD content in patient neutrophil membranes was as low as that of X^0-CGD patients, suggesting complete deletion of FAD. The loss of FAD could not be corrected by adding exogenous FAD to the patient's neutrophil membranes. These results indicate that His^{338} is a critical residue for FAD incorporation into $gp91^{phox}$. This also suggests that incorporation of FAD into $gp91^{phox}$ is related to its stability during synthesis.

More recently, a new case of X^--CGD mutation originating from an 11 bp deletion in the boundary region between the end of exon 12 and the beginning of intron 12 was reported (Stasia et al. 2005). The consequence is a frameshift at Ala^{524} and a stop at position Val^{534}, which is located near the nicotinamide moiety of NADPH binding site (Figure 9). Both the last two mutations (cases 25 and 26) cause the lost of nicotinamide moiety binding site in $gp91^{phox}$.

▸ X^+-CGD

17 mutations have been reported to cause X^+-CGD (Heyworth et al. 2003; Stasia et al. 2005). The major cases are missense mutations, two are small deletions and one is a deletion/ insertion (Table 6). Most of these rare mutations are located in the C-terminal cytosolic region, suggesting that this region is less involved in the stability and the structure of the protein than the N-terminus of $gp91^{phox}$. The functional consequences have been studied in 11 cases (cases 3, 6-14, 17). Yet in the three mutations occurring in Arg54, located in the potential II-transmembrane domain of $gp91^{phox}$ (Figure 7), nearby propionate side chain of the first haem, functional consequences have been studied only in one patient's neutrophils (Cross et al. 1995*a*; Cross et al. 1995*b*). The Arg54Ser mutation affects the function of the haem moiety of cytochrome b_{558}, as indicated by a subtle shift in the optical absorbance properties, a decreased midpoint of one haem from E_{m7} = -265 mV to E_{m7} = -300 mV (Cross et al. 1995*b*), and lack of electron-transfer from FAD moiety to haem. However, the membrane-translocation of $p47^{phox}$ and $p67^{phox}$ occurs normally in activated intact neutrophils from the CGD patient (Cross et al. 1995*a*). These data imply that the electron-transfer from FAD to oxygen requires the two haem groups. Another X^+-CGD mutation (Ala57Glu) is located in the same region as Arg^{54}, the potential II-transmembrane domain of $gp91^{phox}$ (Ariga et al. 1993). Nevertheless no functional analysis was performed for this CGD variant.

Only one double mutation (His303Asn/Pro304Arg) in $gp91^{phox}$ has been reported to cause X^+-CGD (Stasia et al. 2002*a*) (Figure 3). This double substitution was identified in $gp91^{phox}$ mRNA and in the *CYBB* gene. The mutation is located in a site close to the putative FAD-binding site domain of $gp91^{phox}$. However a normal level of FAD was found in neutrophil plasma membranes from the patient. This suggests that this mutation has no effect on the site for binding FAD moiety. The mutated $gp91^{phox}$ functioned as a proton channel in Epstein-Barr virus-transformed B lymphocytes (EBV-LB) as the normal control. However, the $p47^{phox}$ and $p67^{phox}$ translocation to the plasma membrane was strongly disrupted, suggesting that these residues are essential for the oxidase assembly. No inhibition of oxidase activity was observed with synthetic peptides corresponding to residues 296-309 of WT or mutated $gp91^{phox}$, indicating that these residues seems not directly involved in the binding of cytosolic components. These data demonstrated that residues 303 and 304 of $gp91^{phox}$ are crucial for the stable assembly of the oxidase complex and for electron transfer, but not for its proton channel activity.

Table 6 Mutations in *CYBB* gene for gp91*phox* that cause X^+-CGD

Case	cDNA nucleotide (or splice site) change	Mutation	Amino acid change	Potential structral / functional domain	Functional analysis			Cellular model	Reference
					Membrane-translocation of p47*phox* and p67*phox*	NADPH-to-FAD	FAD-to-Haems		
1	A172G	Missense	Arg54Gly	II-transmembrane helix					Ariga et al. 1993
2	G173T	Missense	Arg54Met	II-transmembrane helix					Ariga et al. 1998
3	G174C	Missense	Arg54Ser	II-transmembrane helix	Normal		Defective		Cross et al. 1995
4	C182A174C	Missense	Ala57Glu	II-transmembrane helix					Ariga et al. 1993
5	902-916 deleted	Deletion	298-302 deletion						Dusi et al. 1998
6	C919A/C923G	Missense	His303Asn/Pro304Arg		Defective			PLB-985 cells	Stasia et al. 2002
7	C1034A	Missense	Thr341Lys	The isoalloxazing ring of FAD moiety bindingsite (338HPFTLTSA)	Normal				Leusen et al. 2000
8	T1117C	Missense	Cys369Arg		Defective				Leusen et al. 2000
9	G1235A	Missense	Gly408Glu	Pyrophosphate of NADPH binding site (^{405}MLVGAGIGVTPF^{416})	Defective				Leusen et al. 2000
10	C1256A	Missense	Pro415His	Pyrophosphate of NADPH binding site (^{405}MLVGAGIGVTPF^{416})	Normal			PLB-985 cells	Dinauer et al. 1991; Leusen et al. 1994; Segal et al. 1992
11	3' intron 11 ag/gg	Splice site	488-497 deletion	a-helix (484-504)	Normal	Defective		PLB-985 cells	Schapiro et al. 1991; Yu et al. 1999
12	A1511G	Missense	Asp500Gly	a-helix (484-504)	Defective			PLB-985 cells	Leusen et al. 1994; Li et al. 2005
13	1533-1537 AAAGA deleted/CATCTGGG insert	Deletion/ insert	507-509 GlnLysThr deletion/HisIleTrpAla insert	Adenine of NADPH binding site (^{504}GLKQ^{507})	Normal				Azuma et al. 1995
14	T1526G	Missense	Leu505Arg	Adenine of NADPH binding site (^{504}GLKQ^{507})	Diminished	Diminished		PLB-985 cells	Stasia et al. 2005
15	T1621C	Missense	Cys537Arg	Nicotinamide of NADPH binding site (^{535}FLCGPE^{540})					Rae et al. 1998
16	T1649C	Missense	Leu546Pro						Roesler et al. 1999
17	G1712A	Missense	Glu568Lys		Defective				Leusen et al. 2000

An interesting missense mutation (Pro415His) in gp91^{phox}, causing an X^{+}-CGD (Dinauer et al. 1991), is located in a conserved motif (G-X-G-X-X-P) involved in the binding of the pyrophosphate moiety of NADPH (Sumimoto et el. 1992; Segal et al. 1992) (Figure 3, 9). The translocation of p47^{phox} and p67^{phox} to the plasma membranes is not affected in purified neutrophils from the patient (Leusen et al. 1994*a*). While, the binding of the photoaffinity ligand 2-azido-NADP^{+} is decreased in the neutrophil membranes from this patient, indicating that Pro^{415} is directly implicated in the binding of NADPH (Segal et al. 1992).

Recently, Leusen and colleagues (Leusen et al. 2000) discovered four X^{+}-CGD mutations. Three of them (Cys369Arg, Gly408Glu, and Glu568Lys) are associated with a defective translocation of p47^{phox} and p67^{phox} to the plasma membrane. The Gly408Glu mutation is located in the putative pyrophosphate moiety of NADPH binding site (residues 405-416) (Figure 3). The fourth mutation (Thr341Lys) located in the putative FAD-binding domain (^{338}HPFT^{341} motif) of gp91^{phox} leads to a normal cytosolic factors translocation to the membranes. Although no electron transfer occurs in solubilized neutrophil plasma membranes from any of the four patients. The INT reductase activity, detecting the electron transfer from NADPH to FAD, was not performed.

Four X^{+}-CGD mutations (Table 6) are located near or in the putative adenine moiety of the NADPH binding site of gp91^{phox} (residues 504-507) (Rotrosen et al. 1992) (Figure 3, 9). Only one splice site mutation was found in an X^{+}-CGD patient, in which a splice junction mutation results in an in-frame deletion of 30 nucleotides encoding amino acids 488-497 of gp91^{phox} (Schapiro et al. 1991). A detailed functional analysis has been elucidated in transfected X-CGD PLB-985 cells (Yu et al. 1999*b*), which will be discussed in the following part (6. Cellular models). A point mutation (Asp500Gly), identified in an X^{+}-CGD patient leads to a defective translocation of cytosolic proteins to the plasma membranes of the patient neutrophils (Leusen et al. 1994*a*). Another missense mutation (Leu505Arg) has been recently reported (Stasia et al. 2005). This X^{+}-CGD case was reproduced in the PLB-985 cells to investigate the dysfunction of mutated gp91^{phox} as described in the "Cellular models" part. Another X^{+}-CGD mutation results from a deletion/insert mutation (^{507}Gln-Lys-Thr^{509} were converted into His-Ile-Trp-Ala) (Azuma et al. 1995). The translocation of p47^{phox} and p67^{phox} to the patient's neutrophil membrane fraction occurred normally.

The last case of X^{+}-CGD is a substitution Cys537Arg located in the Cys-Gly motif, the potential nicotinamide moiety of NADPH binding site (Rae et al. 1998) (Figure 9). The molecular mechanism of this mutation has not been elucidated.

6. Cellular models

CGD is an excellent model to investigate the NADPH oxidase complex, to identify its cellular components and their roles. In each case, cells from CGD patients have played an important role in the experimental approach to understand molecular mechanisms of NADPH oxidase activation and molecular pathology of CGD. However, mature neutrophils isolated from blood do not proliferate, have an *in vitro* short lifespan and are not readily "transfectable". In addition it is often difficult to get enough total blood from CGD patients to conduct functional analysis of the mutations in purified neutrophils. These weaknesses are

surmounted by using various myeloid (EBV-LB, K562, $CD34^+$, HL-60, PLB-985) and non-myeloid cell lines (CHO, COS7, HEK293, 3T3).

EBV-LB

The Epstein-Barr virus (EBV) is a human lymphotropic herpes virus associated with Burkitt's lymphoma and nasopharyngeal carcinoma. It converts normal human B lymphocytes to immortalized lymphoblastoid lines. The investigation of CGD has been greatly facilitated by the availability of EBV-transformed lymphocyte B (EBV-LB), which has the biochemical and genetic characteristics of neutrophils. B cell lines contain all the known components of NADPH oxidase. These cells produce superoxide in a manner essentially identical to that of neutrophils and other phagocytes (Maly et al. 1988), although at low levels relative to neutrophils (1% of neutrophils' activity) (Volkman et al. 1984). Moreover, EBV-LB cell lines established from CGD patients display the disease phenotype of defective superoxide generation and are deficient in the same NADPH oxidase component missing from neutrophils. EBV-LB cell line provides a valuable model system for the study of CGD.

Firstly, the identification of the molecular defects in CGD neutrophils is often hampered by the limited amount of blood from the patients. The unlimited quantities of EBV-LB lead to a marked improvement in the mutation identification in genes implicated in this disease. Secondly, EBV-LB cells derived from CGD patients can be used directly to explore the defective biochemical mechanism of this disease. For example, proton channel activity of a rare X^+-CGD mutation (His303Asn/Pro304Arg) was measured in this cell line from the patient (Stasia et al. 2002*a*). Thirdly, these cells provide an optimal environment to study the functional correction of the CGD by gene transfer. CGD-derived EBV-LB cell lines have been used as targets for the expression of $p47^{phox}$, $gp91^{phox}$ and $p22^{phox}$ (Thrasher et al. 1992; Porter et al. 1993; Maly et al. 1993). The first gene therapy in EBV-LB deficient in $p47^{phox}$ was realized by the group of Segal (Thrasher et al. 1992). The presence and the activity of the retrovirally encoded $p47^{phox}$ in the transduced cells haven been demonstrated and this restored their capability to generate superoxide. Fourthly, EBV-LB cell lines will serve as a model for studying the intermolecular interactions and the function of the oxidase components. Co-expression of MPR8 and MRP14 (*M*yeloid-*R*elated *P*roteins) in the EBV-LB cells increased the oxidase activity, suggesting that MPR8/MRP14 are the positive factor of the NADPH oxidase (Berthier et al. 2003). In this model, the maturation of $gp91^{phox}$ glycosylation was found to be dependent upon the presence of $p22^{phox}$ (Porter et al. 1994).

However, the EBV-LB cells are neither easily transfected nor efficient for expression of the oxidase proteins, which is associated with its low oxidase activity (De Mendez at al. 1995).

K562 cells

The K562 cell line is derived from a patient with a chronic myelogenous leukemia in blast crisis. It is a highly undifferentiated, multipotent, hematopoietic precursor cell line (De Mendez at al. 1995). After exposure to various stimuli, this cell line undergoes either erythroid, megakaryocytic, or granulocytic differentiation. However, its usefulness is limited by its inability to achieve a state of complete, terminal maturation indistinguishable from its normal counterparts (Tucker et al. 1987).

Undifferentiated K562 cells express endogenous Rac2 and $p22^{phox}$. These easily transfected cells provide an ideal model in which several components of the oxidase can be genetically manipulated and readily expressed. Functional NADPH oxidase has been reconstituted in K562 cells by transfection of $gp91^{phox}$, $p47^{phox}$ and $p67^{phox}$ (De Mendez at al. 1995). This cellular model facilitates the studies on the interactions among several oxidase components. Co-expression of $p47^{phox}$ and $p67^{phox}$ augments Nox1 activity in reconstituted K562 cells (Geiszt et al. 2003*a*), indicating that this cell line can be used to study the homologues of $gp91^{phox}$. K562 cell line has also been used to study the role of homologues of $p47^{phox}$ and $p67^{phox}$ (NoxO1 and NoxA1, respectively). Co-expression of NoxO1 and NoxA1, or NoxA1 and $p47^{phox}$, or NoxO1 and $p67^{phox}$, or $p47^{phox}$ and $p67^{phox}$ could support the PMA-activable oxidase activity in the $gp91^{phox}$-transfected K562. In addition the $p47^{phox}$-$p67^{phox}$ combination presents the maximal oxidase activity, suggesting that they are the optimal factors for $gp91^{phox}$ (Geiszt et al. 2003*a*; Takeya et al. 2003).

▸ $CD34^+$

Although prophylactic antibiotics and interferon γ constitute a cornerstone of CGD treatment and have brought a better outlook, morbidity caused by infections or granulomatous complications remain significant (Weening et al. 1983; Hara et al. 2004). Bone marrow transplantation (BMT) in CGD has been associated with unacceptably high rates of morbidity, mortality, and graft failure, except in the case of HLA-matched sibling donors (Calvino et al. 1996; Ho et al. 1996). An alternative strategy to allogeneic BMT is gene therapy. $CD34^+$ cell line is the possible target for gene therapy. $CD34^+$ cells represent a heterogenous population with only a small number of undifferentiated progenitors. The main biological characteristic of $CD34^+$ cells is their capacity to reconstitute the myelo and lymphopoietic system after a myeloablative treatment. $CD34^+$ peripheral blood progenitors have been used as a target for genetic correction of the two flavocytochrome b_{558} defective forms of CGD. A significant functional correction of the oxidase activity in $gp91^{phox}$- and $p22^{phox}$-deficient phagocytes was developed from transduced $CD34^+$ cells from CGD patients (Li et al. 1994). $CD34^+$ cells purified from GM-CSF-mobilized peripheral blood mononuclear cells of a $gp91^{phox}$-deficient CGD patient, were transduced with a bicistronic retrovirus vector, containing $gp91^{phox}$ and MRD (multidrug resistence gene), and then inplanted in C57BL/6 mice. The results suggest that $gp91^{phox}$ transduced $CD34^+$ cells could be selected by MDR *in vivo* (Sugimoto et al. 2003).

Autologous peripheral blood $CD34^+$ cells collected by apheresis were transduced with $p47^{phox}$-containing retroviral vector and then reinfused in an A47-CGD patient for phase 1 clinical trial (Malech et al. 1997). This constituted the first genetic therapy assay in CGD. Recently a Phase I/II clinical gene therapy essay was conducted for two X-CGD patients suffering from a long history of recurrent and life-threatening bacterial and fungal infections (Ott et al. 2004). G-CSF mobilized $CD34^+$ cells were transduced with a monocistronic $gp91^{phox}$ retroviral vector (about 40% transduction efficiency) and then reinfused to the patients. A significant fraction of gene marked cells has been detected in the peripheral blood of both patients since day +21. Similarily, therapeutically relevant levels of ROS production have been observed. These data suggest that gene therapy is a definitive promising resolution to cure CGD.

PLB-985

PLB-985 cell line is a human diploid, myeloid leukemia cell line, obtained from the peripheral blood of a patient with an acute nonlymphocytic leukemia (Tucker et al. 1987). Phenotypically these cells are myelomonoblasts, less mature than the promyelocytes of HL-60 line. They have the capacity for both granulocytic and monocyte/macrophage maturation in the presence of inducing agents. PLB-985 differentiation is associated with increased expression of gp91^{phox}, p22^{phox}, p47^{phox}, p67^{phox} and p40^{phox} (Pedruzzi et al. 2002). X-CGD PLB-985 cell line has been established by inserting a cassette for hygromycin B phosphotransferase expression into the third exon of *CYBB* gene using gene targeting technique (Zhen et al. 1993). Superoxide production was absent in targeted cells after granulocytic differentiation but was rescued by stable transfection and expression of gp91^{phox} cDNA. An X^{+}-CGD mutant (Pro 415His) transfected X-CGD PLB-985 cells express normal levels of gp91^{phox} but fail to generate superoxide, reproducing the phenotype of the patient's neutrophils (case 10, Table 6) (Figure 3). These data indicates that X-CGD PLB-985 cell line provides the advantage of performing reconstitution experiments in a myeloid-cell environment.

This cell line is an excellent cellular model for studying the relationship between structure and function of gp91^{phox}. The role of four regions of gp91^{phox} on the NADPH oxidase activation has been elucidated in this cellular model by mutagenesis approach. Replacement of nonpolar by polar or charged residues in the C-terminal region of gp91^{phox} ^{559}RGVHFIF^{565} inhibited the oxidase activity, but also decreased the expression of gp91^{phox}, suggesting that overall protein structure was perturbed. No stable gp91^{phox} was detected upon deletion of the 11 terminal amino acid residues (Zhen et al. 1997), indicating that the C-terminal region of gp91^{phox} is essential for the protein stability. In the hydrophilic, polybasic domain of gp91^{phox} encompassed by residues 86-102 (B-loop, Figure 3), Arg^{91} and Arg^{92} were found to be essential for cytochrome b_{558} function and for the interaction of gp91^{phox} with the oxidase cytosolic components in granulocytic-differentiated transfected PLB-985 cells (Biberstine-Kinkade et al. 1999). The second intracellular loop (D-loop) of gp91^{phox} (^{191}TSSTKTIRRS^{200}) and especially the charged amino acids Lys^{195}, Arg^{198} and Arg^{199}, are implicated in electron transfer from FAD to the haems but are not involved in the assembly process. While the α-helical loop containing residues 484-504, which is proposed to be over the NADPH binding site (Taylor et al. 1993), is indispensable for the oxidase activity, the oxidase complex assembly and the electron transfer from NADPH to FAD (Li et al. 2005). Indeed the role of His^{101}, His^{115}, His^{209} and His^{222} on oxidase activation, haem binding and cytochrome b_{558} maturation were found by directed mutagenesis and stable transfection in X-CGD PLB-985 cells (Biberstine-Kinkade et al. 2001).

The cytochrome b_{558} synthesis process and the respective role of gp91^{phox} and p22^{phox} in this process have been investigated in PLB-985 cell line (Yu et al. 1999*a*). Haem synthesis inhibitory study using succinyl acetone in PLB-985 cells demonstrated that the acquisition of haem by gp65 (65-kDa precursor of g91^{phox}, synthesized in the endoplasmic reticulum as a high-mannose precursor) (Yu et al. 1999*a*) preceded and was necessary for the binding of p22^{phox} (Deleo et al. 2000). The heterodimer formation is not a co-translational process, and haems insertion is a determinant event in the formation of a stable heterodimer but appears not to affect the stability of gp65. DeLeo *et al.* found that the acquisition of haem by gp65 is a

prerequisite for the formation of gp65-p22^{phox} heterodimer early in flavocytochrome b_{558} biosynthesis (DeLeo et al. 2000).

This model is highly useful to modelize X^+-CGD cases to study the impact of mutations on molecular mecanisms of the oxidase complex's dysfunction. The first functional analysis of an X^+ CGD case in these cells was a splice site mutation Δ488-497-gp91^{phox} (Schapiro et al. 1991). Indeed detailed functional analysis of this X^+-CGD mutant gp91^{phox} (Δ488-497) could not be performed due to the death of the patient (case 11, Table 6). This mutation is localized in the 20-amino acids loop forming an α-helix (residues 484-504) over the NADPH binding pocket in the proposed 3D model of the C-terminal tail of gp91^{phox} (Taylor et al. 1993) (Figure 3). During the oxidase activity, this loop may be drawn aside by the interaction with cytosolic components to give the NADPH access to its binding site. However the Δ488-497 deletion in this C-terminal region of gp91^{phox} seems not to influence cytosolic factors translocation to the plasma membranes but alters the electron transfer from NADPH to FAD [iodonitrotetrazolium (INT) reductase activity]. On the contrary a point mutation (Asp500Gly), identified in an X^+-CGD patient (case 12, Table 5) leads a defective translocation of cytosolic proteins to the plasma membranes of defective neutrophils (Leusen et al. 1994*a*). To confirm the importance of this domain on oxidase assembly, the authors tested the effect of synthetic peptides corresponding to residues 491-504 of gp91^{phox} on the translocation of p47^{phox} and p67^{phox} in the CFS assay with membranes and cytosol from control neutrophils. Interestingly, the wild-type peptide strongly inhibited translocation and superoxide generation, whereas the peptide containing the substitution (Asp500Gly) was much less effective.

We used the X-CGD PLB-985 cells to study two cytosolic regions of gp91^{phox} (Li et al., 2005) and notably the α-helical loop (residues 484-504) (Chapitre 2) (Figure 3). In this work the Asp500Gly mutation was also reproduced and exhibited the same phenotype as the patient's neutrophils. These results highlight the essential role played by the α-helical loop (residues 484-504) (Figure 3), consistent with the model of Taylor *et al.* (Taylor et al. 1993). We pointed out that this region is essential for a correct assembly of the oxidase complex during the time course of oxidase activation. This assembly is intimely related to the electron transfer from NADPH to FAD as proposed by the model of Taylor and Segal.

Recently a new X^+-CGD case resulting to a Leu505Arg missense mutation (case 14, Table 6) diagnosed in our lab, was studied after reconstitution in the X-CGD PLB-985 cell line (Stasia et al. 2005, Chapitre 3). Leu^{505} is supposed to be located in the adenine of NADPH binding site of gp91^{phox} (^{504}GLKQ^{507}) closed to the α-helical loop (residues 484-504) (Rotrosen et al. 1992) (Figure 3, 9). Yet this amino acid is essential for the oxidase activation, Leu^{505} seems not to be directly implicated in the binding of NADPH (Chapter 3). The increased quantity of p67^{phox} could restore NADPH oxidase activity in the simplified cell-free-system, suggesting that this mutation perturbs the interaction between gp91^{phox} and p67^{phox}. In addition Leu505Arg mutation could alter the α -helical loop position affecting NADPH access to its binding site.

Finally X-CGD PLB-985 cells were used to study the impact of the double missense mutation His303Asp/Pro304Arg (Stasia et al. 2002*a*) and each single mutation on oxidase activity and assembly (case 6, Table 6). We found that even if the His303Asn mutation has a more severe inhibitory effect on NADPH oxidase activity and assembly than the Pro304Arg

mutation, neither mutation can be considered as a polymorphism in the *CYBB* gene (Bionda et al. 2004).

In addition the X-CGD PLB-985 cell line has been used to study the homologues of gp91^{phox}. Transduction with retrovirus encoding Nox1 restored activation and differentiation-dependent superoxide production in X-CGD PLB-985 cells, indicating close functional similarities to the phagocyte oxidase (Geiszt et al. 2003*b*). This observation suggests that Nox1 or other Nox proteins can compensate for the gp91phox-deficiency in X-CGD, and that targeted up-regulation of Nox proteins in phagocytic cells may partially correct the CGD phenotype.

The involvement of cytosolic phospholipase A2 and its metabolite the arachidonic acid in regulation of NADPH oxidase have been investigated in PLB-985 cells. The results establish an essential and specific physiological requirement of cytosolic phospholipase A2-generated arachidonic acid in activation of electron transfer through the FAD reduction center of the oxidase (Pessach et al. 2001), and in the activation of proton flux through the N-terminal fragment of gp91^{phox} (residues 1-230) (Figure 7) (Mankelow et al. 2003*a*).

▸ CHO

CHO (*C*hinese *h*amster *o*vary) cell line was initiated from a biopsy of an ovary of an adult Chinese hamster. Northern blot analysis of CHO cells demonstrated the absence of p22^{phox} mRNA (Biberstine-Kinkade et al. 2002). It suggests that this cell line maybe an ideal model for structural-functional study of p22^{phox}. Currently, there are conflicting views about the distribution, the exact location and the coordination of haems within the flavocytochrome b_{558}. Quinn *et al.* (Quinn et al. 1992*a*) suggested that both gp91^{phox} and p22^{phox} bind haems and proposed that one haem binds exclusively to gp91^{phox}, whereas the other one is shared between gp91^{phox} and p22^{phox}. P22^{phox} has only a single invariant histidine residue (His^{94}). The group of Dinauer found that expression of either His94Leu p22^{phox} or wild type p22^{phox} promoted maturation of transgenic gp91^{phox} from its 65-kDa precursor to its fully glycosylated form in CHO cells (Biberstine-Kinkade et al. 2002). This suggests that fully glycosylation of gp91^{phox} is dependent on the presence of p22^{phox} in this cell line. This mutagenesis study in CHO cells demonstrated that His^{94} in p22^{phox} is not required for haem binding or function of flavocytochrome b_{558} in the NADPH oxidase.

CHO cell line is the most important cellular system for the study of a proton channel associated with the oxidase activity. The group of Henderson found a lot of results from this cellular model. They have proposed that gp91^{phox}, the large subunit of the NADPH oxidase cytochrome b_{558}, was the arachidonate activable proton channel of human neutrophils (Henderson et al. 1995). Transfection of the N-terminus of gp91^{phox} (residues 1-230) in CHO cells demonstrated that it contains all the requirements to function as the oxidase-associated proton channel (Henderson et al. 1997) (Figure 7). A positive correlation between the expression of gp91^{phox} and the presence of a voltage-gated H^+ current was found in the CHO cells by using the whole cell configuration of the patch clamp technique (Henderson et al. 1999). This confirms that gp91^{phox} is a voltage-gated proton pathway. Stable CHO cell lines were established which expressed full-length gp91^{phox} in which His^{111}, His^{115}, and His^{119} had been mutated to Leu (CHO91H111/115/119) and in which His^{115} had been mutated to Leu (CHO91H115) (Mankelow et al. 2003*b*). The expression of gp91^{phox} and its cellular

localisation in these cell lines were comparable between the wild-type and mutant gp91^{phox}. Whereas both the arachidonate-activated influx and efflux of protons were abolished in the mutated CHO cell lines, suggesting that His^{115} is absolutely required for the proton conduction by gp91^{phox}. The requirement for His^{119} in the conduction of protons was confimed by the same group using similar methods (Mankelow et al. 2004). Taken together, the proton conduction through gp91^{phox} requires His^{115} and His^{119}.

HEK293

HEK293 cells were generated by transformation of *h*uman *e*mbryonic *k*idney cell culture with sheared adenovirus 5 DNA and subsequently demonstrated to be a useful cell type to produce adenovirus, other viral vectors, and effectively glycosylated human recombinant proteins. This cell line expresses endogenous p22^{phox} (Maturana et al. 2001; Ambasta et al. 2004). In gp91^{phox}-transfected HEK293 cells, the haem spectral signature was clearly visible and the size of the expressed protein was close to 90 kDa (Maturana et al. 2001). These data suggest that gp91^{phox} protein is able to mature to its fully glycosylated state. Interestingly, the mutant His115Leu, which is unable to bind the haem prosthetic group, has no influence on the glycosylation of gp91^{phox} (Figure 7). It suggests that the fully glycosylation of gp91^{phox} occurs in the complete absence of haem insertion in the transfected HEK293 cells. However, the haem insertion is critical for the formation of stable heterodimers between gp91^{phox} and p22^{phox}, a process that is required for the insertion of cytochrome b_{558} into the plasma membrane of phagocytes (Yu et al. 1997; DeLeo et al. 2000). These results suggest that the maturation of gp91^{phox} in myeloid cell line is not exactly comparable to that occurs in nonphagocytic cell line. In the HEK293 cellular model, His^{115} of gp91^{phox} was found to be involved in both haem ligation and proton conduction (Maturana et al. 2001).

HEK293 is also an ideal model for the study of the homologues of gp91^{phox}. More recently, this cellular system has been used to study the interaction of novel Nox proteins with p22^{phox} (Ambasta et al. 2004), interaction of two regulating factors of Nox1 (NoxO1 and NoxA1) with Nox1 and gp91^{phox} (Banfi et al. 2003), the structure-function in the NoxO1 (Cheng et al. 2004), and the cross-talk between Nox3 and the regulating factors of Nox1 and gp91^{phox} (Banfi et al. 2004). Immunoprecipitation from transfected HEK293 cells revealed co-precipitation of native p22^{phox} with cyan fluorescent protein-tagged Nox1, Nox2, and Nox4, suggesting that there is direct interaction of the Nox proteins with p22^{phox} (Ambasta et al. 2004). Co-expression of Nox1 with NoxO1 and NoxA1 led to stimulus-independent high level of superoxide generation, indicating that Nox1 is a superoxide-generating enzyme that is activated by its partners (Banfi et al. 2003). A point mutation in the N-terminal PX domain (Arg40Gly) of NoxO1 decreased lipid binding resulting in cytosolic localization and inhibited NoxO1-activation of Nox1 in transfected HEK293 cells. This demonstrates that the activation of Nox1 with NoxO1-NoxA1 is partially mediated by the binding of NoxO1 PX domain to membrane lipids (Cheng et al. 2004).

COS-7

COS-7 cell line is derived from the CV-1 cell line by transformation with an origin defective mutant of SV40 which codes for wild type T antigen. COS-7 cells express endogenous Rac1 and much more PKC-α, PKC-ι, and PKC-ζ than human neutrophils but has

undectable PKC-βII and low levels of PKC-δ (Price et al. 2002). Neither gp91^{phox} nor p22^{phox} mRNA expression was detected by Northern blot analysis of COS-7 cells (Yu et al. 1997). Maturation of high mannose carbohydrates to complex oligosaccharides on gp91^{phox} can occur in the absence of p22^{phox} in gp91^{phox}-transfected COS-7, in which a characteristic cytochrome b_{558} haem spectrum was observed (Yu et al. 1997). However, the mRNA of p22^{phox} was detected by RT-PCR in 2 cell lines of COS-7 from different origins in our laboratory. Furthermore, the protein p22^{phox} was also observed by Western blotting as well as FACS by Tissot Dupont and Stasia (unpublished results). The predominant form of gp91^{phox} in its transfected COS-7 appears to be the 58- or 65-kDa precursor (Yu et al. 1998). However, coexpression of gp91^{phox} and p22^{phox} in COS-7 membranes was required to support superoxide generation in combination with neutrophil cytosol, indicating that the functional assembly of the active NADPH oxidase complex requires both subunits of cytochrome b_{558} (Yu et al. 1998). His^{101}, His^{115}, His^{209} and His^{222} of gp91^{phox} are critical for haem-binding and biosynthetic maturation of cytochrome b_{558} in transfected COS-7 cells (Biberstine-Kinkade et al. 2001).

Transgenic expression of recombinant oxidase subunits (gp91^{phox}, p22^{phox}, p47^{phox} and p67^{phox}) in COS-7 conferred high-level of superoxide production and was activated by either PMA or arachidonic acid (Price et al. 2002). Expression of p47^{phox} Ser303Ala/Ser304Ala or Ser379Ala phosphorylation-deficient mutants in gp91^{phox}/p22^{phox}-transfected COS-7 cells resulted in significantly impaired NADPH oxidase activity (Price et al. 2001). The mutant Val204Ala of p67^{phox}, located in the p67^{phox} activation domain (figure 5), abrogates superoxide production in transfected COS-7 cells, confirming the results obtained in the CFS assay that residues 199-213 of p67^{phox} are essential for the activation of the oxidase complex (Figure 5). Furthermore, expression of transgenic Rac T17N mutant or RhoGDI significantly inhibited both PMA- and arachidonic acid-induced superoxide generation in COS-*phox* cells, suggesting that Rac activation and membrane translocation are important for assembly of the active NADPH oxidase complex in whole COS-7 cells. Thus, the COS-*phox* system is believed to be a useful model for studying functional domains in oxidase components necessary for assembly and activation of this enzyme in intact cells.

COS-7 cell line has been also used in the proton channel study. The transient expression of gp91^{phox} induced large currents in COS-7 cells, suggesting that gp91^{phox} acts as a voltage-gated channel (Maturana et al. 2001). Morgan et al found that there was an absence of proton channels in COS-7 cells expressing the oxidase components, indicating that gp91^{phox} does not function as a proton channel with a demonstrably functional oxidase (Morgan et al. 2002). However, Murillo et al. found that the absence of proton current in COS-7 cells expressing gp91^{phox} results from a failure in the expressed protein to be localised in the plasma membranes. Gp91^{phox} appears to lack extensively glycosylation in COS-7 cells, which may prevent the expressed protein leaving the endoplamic reticulum and hence altering its membranous localisation.The expression of gp91^{phox} in COS-7 was found to be associated with the presence of an outward proton currents (Murillo et al. 2004).

COS-7 cell line was also used to study the homologues of p47^{phox} and p67^{phox} (Takeya et al. 2003). Co-expression of NoxA1-NoxO1 or NoxO1-p67^{phox} in the gp91^{phox}-transfected COS-7 could support the PMA-activated oxidase (Nox2) activity; And this co-expression is

functional for the activity of Nox1 in transfected COS-7 cells, suggesting that the existence of a common mechanism underlying the activation of Nox famly oxidases.

7. The objectives of the work

The NADPH oxidase is a multi-protein complex which becomes activated when cytosolic components ($p47^{phox}$, $p67^{phox}$ and $p40^{phox}$) reach the plasma membranes of phagocytes to bind its membranous redox element, the cytochrome b_{558} which is composed of two subunits, $gp91^{phox}$ or Nox2 and $p22^{phox}$. It is only in this assembled activated state of this enzyme that the electron transfer occurs through the cytochrome b_{558} from NADPH to molecular oxygen via FAD. This highlights that the regulation of the NADPH oxidase activity depends on protein-protein interactions and that is intimately related to the electron transfer which generates superoxide anions.

One way to investigate the NADPH oxidase activation process is to study its dysfunction in an orphan genetic disease, the chronic granulomatous disease. One variant, the X^+ CGD, is particularly interesting to study because it is characterized by a normal expression of the mutated $gp91^{phox}$ protein which is non functional. It is easy to understand that a relation between a mutated region of $gp91^{phox}$ and its specific function could be established by this way. Unfortunately neutrophils purified from the patient's blood are often inadequate to study molecular mechanisms that provoke the dysfunction of NADPH oxidase in this variant.

The aim of this work was to study the role of some specific regions of $gp91^{phox}$ using directed mutagenesis and stable transfection approaches in a useful cellular model performed by Dinauer and coworkers (Zhen et al. 1993), the X-CGD PLB-985 cells. PLB-985 cells are pro-myelocytic cells which can be differentiated in neutrophils by specific agents. The knock-out cells were obtained by *CYBB* gene targeting leading to a cell line resembling to neutrophils from an X^0-CGD patient.

1) An X^+-CGD case due to a double missense mutation His303/Pro304 (Stasia et al. 2002*a*) has been reproduced in the X-CGD PLB-985 cell model. The aim was to elucidate the impact of the double mutation and of each one on the NADPH oxidase activation process (Chapter 1).

2) The second objective of this work was to investigate the role of two regions of Nox2: the second intracytosolic loop (D-loop) (^{191}TSST**K**TI**RR**S^{200}) and a C-terminal cytosolic domain (^{484}**D**ESQAN**H**FAVHH**D**EEK**D**^{500}). These charged regions are particularly conserved in the Nox family especially the underlined amino-acids. The D-loop is located near the transmembrane α helice V, implicated in the haem-binding (His^{209} and His^{222}). These data suggest that this domain is very important for the activation and/or the structure of the NADPH oxidase. In addition this loop has never been studied.

According to the proposed 3D model of the C-terminal cytosolic tail of $gp91^{phox}$ (Taylor et al. 1993), the second studied domain forms an α-helical loop and lies over the NADPH binding cleft in the resting state. Upon activation, this loop interacts with the oxidase cytosolic components and moves aside to allow NADPH to access its binding site in $gp91^{phox}$. Several works have been done in this region (Leusen et al. 1994; Yu et al. 1999*b*; Tsuchiya et al. 1999), but results are very controversial. In addition the α-helical loop is only found in Nox/Duox family and FRE1, suggesting that this loop has a special function in these proteins.

A second X^+-CGD case due to a missense mutation Asp500Gly localised in the α-helical loop, was also reproduced and studied in the X-CGD PLB-985 cell model (Leusen et al. 1994). Moreover a double missense mutation RR9192EE in the B-loop previously studied (Biberstine-Kinkade et al. 1999) was replicated in this cellular model to validate our methodology (Chapter 2).

3) The last studied X^+ CGD mutation was the Leu505Arg substitution (Stasia et al. 2005). Leu505Arg is located on the potential adenine binding site (^{504}GLKQ^{513}) and is at ending of this α-helix loop as previously described. This residue is heavily conserved in the Nox/Duox family, suggesting that it plays a similar role in this family. The impact of this mutation on NADPH oxidase activation process, was investigated in the X-CGD PLB-985 cell model (Chapter 3).

4) Our fourth objective was to found the defect in the synthesis and/or maturation of the cytochrome b_{558} in an X^- CGD case (Roesler et al. 1996) due to a missense mutation Ser193Phe located on the D-loop (cf Chapter 2). The work was done using two cellular model, the X-CGD PLB-985 and the COS-7 cells, the first was devoid of $p22^{phox}$ whereas the second expresses it. The aim was to study the influence of the presence of $p22^{phox}$ in the cytochrome b_{558} synthesis (Chapter 4).

Introduction

Les polynucléaires neutrophiles (PMN) sont impliquées dans la défense immunitaire non spécifique de l'hôte contre les agents pathogènes (bactéries, champignons). Lors d'une infections, les PMN circulant sont attirés vers le foyer infectieux par des agents chimiotactiques (le formyl-méthionyl-leucyl-phénylalanine ou fMLP, le composant C5α du complément, l'interleukine 8, les leukotriènes B4), sécrétés par les bactéries ou générés par l'hôte. Les neutrophiles reconnaissent les bactéries préalablement « opsonisées », grâce aux récepteurs membranaires spécifiques des opsonines (récepteurs aux immunoglobulines ou Ig, récepteur du complément). Les bactéries sont ensuite phagocytées avec formation d'un phagosome (Figure 1). Parallèlement à cette phagocytose, des lysosomes cytosoliques (granules azurophiles, spécifiques, vésicules de sécrétion) migrent vers le phagosome, fusionnent avec lui pour déverser les hydrolases et autres enzymes lysosomiales, protéines cathioniques qu'ils contiennent, à l'intérieur du phagosome pour digérer la bactérie. C'est le stade du phagolysosome. Le phénomène de phagocytose s'accompagne d'une consommation d'oxygène intense. L'augmentation de la respiration des neutrophiles après incubation avec des bactéries a été observée pour la première fois en 1933 par Balbrige et Gérard (Balbrige et al. 1933). L'origine de cette respiration est montrée en 1959, lorsque Sbarra et Karnovsky découvrent que l'augmentation de la consommation d'oxygène est résistante aux inibiteurs conventionnels de la respiration mithochondriale comme le cyanure (Sbarra et al. 1959). Cette explosion respiratoire est à l'origine de la bactéricidie des neutrophiles (Selvaraj et al. 1966). La NADPH oxidase est responsable de la réaction primaire de consommation d'oxygène. Un défaut de fonctionnement de la NADPH oxidase se caractérise par une maladie orpheline héréditaire grave appelée la granulomatose septique chronique (CGD).

1. La production de dérivés toxiques de l'oxygène (ROS)

La NADPH oxydase catalyse la réduction de l'oxygène moléculaire en ions superoxyde en utilisant le nicotinamide adénine dinucléotide phosphate réduit (NADPH) :

$$NADPH + 2O_2 \xrightarrow{\text{NADPH oxidase}} NADP^+ + H^+ + 2O_2^{-\bullet}$$

Les ions superoxyde sont des molécules instables qui vont être transformés en divers composés à pouvoir bactéricide. Ils subissent ensuite une dismutation spontanée ou sont transformé en peroxyde d'hydrogène grâce à la superoxyde dismutase (SOD).

$$O_2^{-\bullet} + O_2^{-\bullet} + 2H^+ \xrightarrow{\text{SOD}} O_2 + H_2O_2$$

La myeloperoxydase (MPO) présente dans les granules azurophiles des neutrophiles se déverse dans la vacuole phagocytaire et catalyse la réaction :

$$H_2O_2 + Cl^- + H^+ \xrightarrow{MPO} H_2O + HOCl$$

L'acide hypochloreux (HOCl) peut réagir avec des amines pour donner des chloramines dont certaines sont extrêmement toxiques pour la bactérie:

$$HOCl + R\text{-}NH2 \longrightarrow R\text{-}NHCl + H_2O$$

Les ions superoxyde et le peroxyde d'hydrogène sont modestement réactifs, ils peuvent donner naissance au radical hydroxyle ($OH^{\bullet}$) en présence de métaux.

$$H_2O_2 + OCl^- \longrightarrow {}^1O_2 + H_2O_2 + Cl^-$$

La destruction des bactéries dépend de tous ces dérivés toxiques de l'oxygène, mais particulièrement des ions hypochlorites et des chloramines.

La production de dérivés réactifs de l'oxygène est un processus extrêmement contrôlé. La catalase et la glutathion peroxydase (GSH-PO) composent le système de détoxification, contre une accumulation en peroxyde d'hydrogène :

$$H_2O_2 + H_2O_2 \xrightarrow{catalase} H_2O + O_2$$

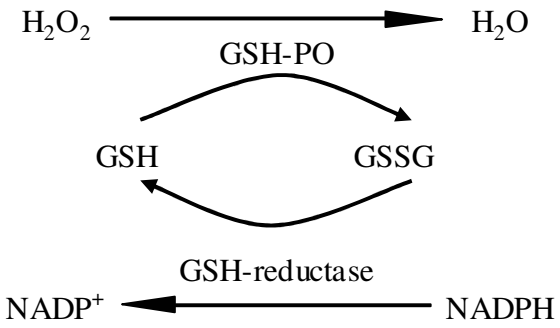

2. NADPH oxidase

La NADPH oxidase est un complexe multi-protéique enzymatique, composée d'un élément redox, le cytochrome b_{558} situé dans la membrane plasmique, une protéine membranaire Rap 1A, et de facteurs solubles $p47^{phox}$, $p67^{phox}$, $p40^{phox}$, et Rac, localisés dans le cytoplasme des phagocytes au repos. L'activation du système passe par l'assemblage des facteurs cytosoliques au niveau du cytochrome b_{558} membranaire, ce qui aboutit à la configuration active de la NADPH oxydase pour produire des ions superoxyde (Figure 2).

2.1 Le Cytochrome b_{558}

Le cytochrome b_{558} est une protéine membranaire intégrale composée de deux sous-unités distinctes α ($p22^{phox}$) et β ($gp91^{phox}$ ou Nox2), dont la stœchiométrie serait de 1 :1 (Huang et al. 1995; Wallach et al. 1996). Dans les cellules au repos, 85% du cytochrome b_{558} est localisé dans la membrane des granules spécifiques, le restant étant contenu dans la membrane plasmique (Borregaard et al. 1983). Après stimulation des neutrophiles, le cytochrome b_{558} des granules se retrouve au niveau de la membrane plasmique (Morel et al. 1985).

- **Gp91^{phox}**

Gp91^{phox} est une glycoprotéine de 570 acides aminés, codée par le gène *CYBB* comportant 13 exons et localisé sur le bras court du chromosome X (Xp21.1) (Table 1) (Royer-Pokora et al. 1986). Le profil d'hydrophobicité prédit la présence de six hélices transmembranaires situées du côté N-terminal, et une région cytosolique du côté C-terminal pouvant se décomposer en 3 zones intracytosoliques : la boucle B ^{70}PVCRNLLSFLRGSSACCSTRIRRQLDRNLTFHK^{102}, la boucle D ^{191}TSSTKTIRRS^{200} et la partie la plus C-terminale contenant les sites potentiels de fixation du NADPH et du FAD (Vignais 2002) (Figure 7). Il est à noter que la partie la plus N-terminale ^{1}MGNWVAVNEGL^{11} est également intracytosolique (Paclet et al. 2005). Les histidines (101/115 et 209/222) situées dans deux passages transmembranaires III et V, sont impliquées dans la liaison de deux hèmes. Gp91^{phox} est synthétisé sous forme d'un précurseur de 65-kDa partiellement glycosylé dans le réticulum endoplasmique. Elle subit ensuite une maturation dans l'appareil de Golgi pour devenir une protéine hautement glycosylée de 91-kDa (Porter et al. 1994 ; Yu et al. 1997). Cette maturation nécessite l'incorporation des hèmes dans le précurseur de 65-kDa et la présence de la protéine p22^{phox} (Yu et al. 1999). Trois asparagines (Asn^{132}, Asn^{149}, Asn^{240}) situées dans les deuxième (la boucle C) et troisième boucles (la boucle E) extracellulaires, sont les sites de glycosylation de la protéine (Wallach et al. 1997).

La comparaison de la séquence de la partie C-terminal de gp91^{phox} avec celles de membres de la famille des ferrédoxines NADP^{+} réductases (FNR) ont montré deux sites potentiels de liaison du FAD ^{338}HPFTLTSA^{345} et ^{355}IRIVGD^{360} (Segal et al. 1992 ; Rotrosen et al. 1992 ; Sumimoto et al. 1992 ; Vignais 2002) ainsi que 4 régions potentielles de liaison du NADPH (Figure 9) :

1) Une région (^{405}MLV*GA*G*IG*VTPF^{416}) riche en glycine qui formerait des liaisons hydrogène avec la partie pyrophosphate du NADPH, elle contient le motif Gly-X-Gly-X-X-Pro.
2) Un domaine (^{442}Y*W*LCR^{446}) contenant une tyrosine très conservée qui formerait une liaison hydrogène avec le ribose du NADPH.
3) La séquence (^{504}GLKQ^{507}) qui formerait une liaison hydrogène avec l'adénine du NADPH.
4) Un double motif Cys-Gly (^{537}CG^{538} pour gp91^{phox}) qui lierait le nicotinamide du NADPH (Segal et al. 1992 ; Rotrosen et al. 1992 ; Sumimoto et al. 1992 ; Vignais 2002).

Certaines parties cytosoliques de gp91^{phox} sont des sites probables de liaison pour les facteurs cytosoliques du complexe oxydase. L'utlisation d'une banque de peptides ayant une séquence aléatoire et l'action inhibitrice de ces peptides ont permis la mise en évidence de trois domaines cytosoliques polybasiques de gp91^{phox} : ^{87}STRVRRQL^{93}, ^{451}FEWFADLL^{458}, ^{491}FAVHHDEEKDVITG^{504} et ^{555}ESGPRGVHFIF^{565} (Leusen et al. 1994 ; DeLeo et al. 1995 ; Park et al. 1997). Par mutagénèse dirigée, deux résidus Arginine de la boucle intracytosolique B en position 91 et 92 ont été montrés comme essentiels à l'activité et à l'assemblage du complexe oxidase (Biberstine-Kinkade et al. 1999). En utilisant la même approche, le rôle des acides aminés chargés (Asp^{484}, His^{490}, Asp^{500}) de la boucle C-terminale formant une hélice α (Taylor et al. 1993) a également pu être mis en évidence dans l'assemblage du complexe oxydase et le transfert électronique du NADPH vers le FAD (Li et al., 2005). Enfin l'analyse

fonctionnelle de cas de CGD X^+ résultant de mutations faux-sens dans la partie C-terminale, ont permis de confirmer l'importance de cette région dans la liaison des facteurs cytosoliques (Leusen et al. 1994, Stasia et al. 2002, Bionda et al. 2004, Li et al. 2005).

- **p22*phox***

La protéine p22*phox* contient 195 acides aminés et est codée par le gène *CYBA* comportant six exons et localisé sur le bras long du chromosome 16 (16q24) (Dinauer et al. 1990) (Table 1, Figure 3). Le profil d'hydrophobicité suggère deux passages transmembranaires et une partie cytosolique du côté C-terminal, qui possède une région riche en proline (PRR), entre les acides aminés 149 et 162. Lors de l'activation du complexe, la région PRR, contenant ^{156}PPRPP^{160} et ^{177}GGPPGGP^{183}, intergit avec les domaines SH3 de la protéine p47*phox* préalablement phosphorylée (Leto et al. 1994). D'autres auteurs prévoient 4 passages transmembranaires de p22*phox* (Heyworth et al. 2003) (Figure 3).

2.2 Facteurs cytosoliques

- **p47*phox***

P47*phox* est une protéine de 390 acides aminés codée par le gène *NCF1* (*N*eutrophil *C*ytosolic *F*actor 1) comportant 11 exons et situé sur le bras long du chromosome 7 (7q11.23) (Lomax et al. 1989) (table 1, Figure 4). Elle possède deux domaines SH3 (*S*rc *h*omology domain *3*) (acides aminés 156-215 et 226-285) (Takeya et al. 2003; Massenet et al. 2005), un domaine PX (acides aminés 4-128) capables de se lier aux phosphatidyl inositides, un domaine AIR (*a*uto*i*nhibitory *r*egion) contenant de nombreux sites de phosphorylation (sérines), un motif polyproline (acides aminés 360-369) interagissant avec le domaine SH3 de p67*phox*. P47*phox* est responsable du transport de la protéine p67*phox* à la membrane au cours de l'activation du complexe oxydase. En l'absence de p47*phox*, p67*phox* n'est pas transloquée à la membrane alors qu'en l'absence de p67*phox*, p47*phox* s'assemble au cytochrome b_{558} (Heyworth et al. 1991). P47*phox* n'est pas indispensable pour reconstituer une activité oxydase *in vitro* (Freeman et al. 1996), elle semble plutôt permettre d'organiser le processus d'activation du complexe oxydase de façon optimale. Elle a été récemment nommée NoxO (Nox organiser) (Banfi et al. 2003; Geiszt et al. 2003; Cross et al. 2004).

- **p67*phox***

La protéine p67*phox* contient 526 acides amines et est codée par le gène *NCF2* comportant 16 exons et situé sur le bras long du chromosome 1 (1q25) (table 1, Figure 5). Le gène a été caractérisé en 1988 (Volpp et al. 1988; Nunoi et al. 1988). Cette protéine possède quatre motifs TPR (*t*ertraco*p*eptide *r*epeat) du côté N-terminal responsable de l'interaction avec la protéine Rac (Koga et al. 1999), un domaine activateur (acides aminés 199-213) (Takeya et al. 2003) indispensable à l'initiation du transfert d'électrons au niveau du cytochrome b_{558} (Han et al. 1998), deux domaines SH3 (acides aminés 240-299 et 457-518) (Takeya et al. 2003), un motif PB1 (*p*hox and *b*emp*1* domain) responsable de l'interaction avec le domaine PB1 de p40*phox* (Kuribayashi et al. 2002). Elle a également un site potentiel de liaison du NADPH (Smith et al. 1996). Contrairement à p47*phox*, p67*phox* est indispensable pour reconstituer une activité NADPH oxydase en système acellulaire (Vergnaud et al. 2000)

- **p40^{phox}**

P40^{phox} , protéine de 339 acides amines et codée par le gène *NCF3* qui comporte 10 exons et est situé sur le bras long du chromosome 22 (22q13.1) (Someya et al. 1993) (table 1, Figure 6). Elle possède un domaine PX capable de se lier aux phosphatidyl inositides, un domaine SH3, et un domaine PB1 (ou PC, *p*hox and *C*dc24 domain) interagissant avec le domaine PB1 de protéine p67^{phox} (Figure 12). La fonction exacte de p40^{phox} n'est pas encore connue, considérée par certains comme un régulateur positif ou négatif (Tsunawaki et al. 1996; Sathyamoorthy et al. 1997; Vergnaud et al. 2000).

- **Rac**

Rac est une petite protéine G appartenant à la famille des protéines Rho. Rac1 (ubiquitaire) et Rac2 (retrouvé dans les cellules de la ligne myéloïde) sont deux isoformes de Rac, qui possèdent une séquence peptidique identique à 92% (Abo et al. 1991; Knaus et al. 1991). Dans les cellules au repos, Rac est liée à Rho-GDI dans le cytoplasme (Abo et al. 1991). Lors de l'activation, il échange le GDP contre le GTP, s'associe au niveau du cytochrome b_{558}. Rac se lie probablement à p67^{phox}, entraînant un changement de conformation de la partie C-terminale de p67^{phox}, permettant sa libération du complexe p67^{phox}-p40^{phox} au cytochrome b_{558} (Rinckel et al. 1999).

2.3 Rap1A

Rap1A est une petite protéine G. Elle est associée au cytochrome b_{558} au niveau de la membrane (Quinn et al. 1989). Son rôle régulateur de l'activité NADPH oxidase reste peu connu (Thrasher et al. 1994). L'étude des lymphocytes B-EBV (Maly et al. 1994) ou des cellules HL-60 (Gabig et al. 1995), exprimant des mutants de Rap1A, a montré une inhibition de l'activité oxydase.

3. La granulomatose septique chronique (CGD)

La granulomatose septique chronique (CGD) est une maladie héréditaire rare (prévalence 1 / 250 000), caractérisée par des infections sévères et récidivantes, résultat d'une incapacité des phagocytes professionnels, principalement les polynucléaires neutrophiles, à produire des dérivés oxygénés toxiques, véritables outils de la bactéricidie (Johnston et al. 1977). La CGD est due à un défaut dans quatre gènes *CYBB*, *CYBA*, *NCF1*, *NCF2* codant respectivement les protéines gp91^{phox}, p22^{phox}, p47^{phox} et p67^{phox} du complexe oxydase (Thrasher et al. 1994; Segal 1996; Heyworth et al. 2003) (Table 3). La CGD présente deux modes d'hérédité : une transmission récessive liée à l'X la plus fréquente (60 %) (CGD X) et une autre autosomale et récessive dans laquelle garçons et filles peuvent être atteints (CGD AR).

3.1 CGD X

Quatre polymophismes sont connus dans le gène *CYBB* (Kuribayashi et al. 1996; Heyworth et al. 2001; Jirapongsananuruk et al. 2002) (Table 4). Les mutations à l'origine des CGD X sont très hétérogènes : délétions, insertions, erreur d'épissage, mutations ponctuelles faux-sens ou non-sens (Roos et al. 1996). On différencie trois variantes de la CGD X selon

l'expression de gp91^{phox}. La forme CGD X^0 est caractérisée par une absence des deux sous-unités du cytochrome b_{558} et représente 50% de toutes les formes de CGD (Royer-Pokora et al. 1986; Roos et al. 1996). Dans la forme CGD X$^-$, le cytochrome b_{558} est présent mais en quantité diminuée et l'activité de la NADPH oxydase est soit nulle soit très réduite. Ce variant est rare (5% des cas) et est dû soit à des mutations ponctuelles faux-sens, soit à de petites délétions, soit à des mutations dans la régions promotrice du gène *CYBB* (Heyworth et al. 2001; Stasia et al. 2003). La forme CGD X$^+$ est un variant rarissime (<5%) et généralement due à une mutation faux-sens, entraînant une expression normale de cytochrome b_{558} associée à une activité de la NADPH oxydase complètement abolie (Roos et al. 1996). Seulement 17 mutations dans le gène *CYBB* à l'origine de CGD X$^+$ ont été rapportés dans la littérature (Heyworth et al. 2001; Stasia et al. 2005) (Table 6). Ces mutations sont principalement localisées dans la partie C-terminale de Nox2. Ceci pourrait indiquer que la partie C-terminale de la protéine est une zone fonctionnelle importante et qui interviendrait moins dans la stabilité de la protéine. Cette portion de la protéine possède en effet des sites de liaison pour le FAD et le NADPH et interagit avec les facteurs cytosoliques (Leusen et al. 1994, Leusen et al. 1999).

Cette forme de CGD est très intéressante car elle permet de mieux comprendre le fonctionnement de la NADPH oxydase. En effet les mutations géniques entraînent l'expression de la protéine gp91^{phox} mutée non fonctionnelle. L'étude fonctionnelle de l'impact de ces mutations permettent de faire des liens entre la structure de la protéine et certaines de ses fonctions spécifiques. Quelques exemples de mutations ponctuelles dans les sites de liaison du FAD (Thr341Lys), du NADPH (Gly408Glu, Pro415His), dans des zones d'interactions avec les facteurs cytosoliques (His303Asn/Pro304Arg, Asp500Gly, Leu505Arg), dans le passage transmembranaire II impliqué dans le fonctionnement des hèmes et le passage des électrons du FAD vers l'oxygène (Arg54Ser).

3.2 CGD AR

La CGD AR47^0 est la deuxième forme par ordre de fréquence après la CGD liée à l'X et elle représente 30% des cas de CGD (Table 3). La protéine p47^{phox} est absente et l'activité oxydase est nulle. Dans 94% des cas, cette forme est dûe à une délétion de 2 nucléotides GT dans une répétition de GTGT située au début de l'exon 2 (Casimir et al. 1991; Vazquez et al. 2001). La conséquence est un glissement du cadre de lecture avec apparition d'un codon stop prématuré sur l'acide aminé 51. Un pseudogène de *NCF1* récemment mis en évidence, possède cette mutation (Roelser et al. 2000; Vazquez et al. 2001). Des recombinaisons entre le gène et son pseudogène pourrait être une explication possible à la fréquence d'apparition de cette mutation (Heyworth et al. 2003).

La CGD A67^0 représente 5% des CGD (Table 3). Une seule forme de CGD A67$^-$ est connue. Ce cas est due à une délétion différente sur chacun des allèles : une de 11 à 13 kb pour laquelle on ne retrouve pas de protéine correspondante et une de 3 nucléotides qui entraîne la perte de la lysine 58. Cette mutation semble être associée à une diminution de la liaison de p67^{phox} à la protéine Rac. Cette dernière interagirait en effet avec les 199 premiers acides aminés de p67^{phox}. La lysine 58, située dans un des domaines TRP de p67^{phox} (Figure 5) serait donc un site de liaison pour la protéine Rac ou serait un acide aminé important pour maintenir la partie N-terminale de p67^{phox} dans une conformation adaptée à la liaison avec

Rac. L'absence d'interaction entre $p67^{phox}$ et Rac perturberait l'assemblage de la NADPH oxydase (Leusen et al. 1996).

La CGD $A22^0$ est également une forme rare (5%) (Table 3). Un seul cas de CGD $AR22^+$ a été rapporté. Il s'agit chez ce patient d'une mutation ponctuelle à l'origine du remplacement d'une proline en position 156 par une glutamine (Figure 3). Cette mutation intervient dans une région riche en proline de $p22^{phox}$ qui est impliquée dans la liaison avec un domaine SH3 de la protéine $p47^{phox}$. L'abolition de l'activité NADPH oxydase chez ce patient serait donc due à un défaut de liaison des facteurs cytosoliques avec le cytochrome b_{558} (Dinauer et al. 1991, Leusen et al. 1994) et plus particulièrement au niveau de $p22^{phox}$. Cette substitution est la première mutation connue qui perturbe une interaction SH3-proline entraînant une maladie génétique (Roos et al. 1996*a*).

4. Modèles cellulaires d'étude du complexe oxydase

Les modèles cellulaires d'étude de la NADPH oxydase ont été développés d'une part pour comprendre les mécanismes d'activation du complexe et d'autre part, pour réaliser le diagnostic moléculaire des mutations responsables de la CGD. Ils ont également été très intéressants pour réaliser les premiers essais de thérapie cellulaire *ex vivo* qui ont permis ensuite de faire les premiers pas vers la thérapie génique. Dans certains cas, les mutations humaines sont reproduites dans ces modèles et l'impact de ces mutations sur les mécanismes d'assemblage du complexe oxydase est étudié.

Enfin, l'étude du rôle des analogues de certaines protéines du complexe oxydase tels que Nox1, NoxO1 et NoxA1 a été réalisée grâce à ces modèles.

4.1 Les lymphocytes B immortalisés par le virus d'Esptein-Barr (LB-EBV)

Les lymphocytes B possèdent un complexe NADPH oxydase structuralement et immunologiquement identique à celui des neutrophiles. Cependant la production d'ions superoxyde représente moins de 1% de celle des neutrophiles stimulés par le PMA (Volkman et al.1984). Dans les lymphocytes B de patients atteints de CGD, l'activité oxydase est abolie comme dans les PNN. Ces cellules sont facilement immortalisables grâce au virus Epstein Bar (Maly et al. 1988). Ainsi immortalisés ces cellules constituent un matériel de choix pour :

1) pérenniser les mutations géniques des malades afin de les identifier (Stasia et al. 2005).
2) analyser les mécanismes moléculaires de fonctionnement ou de dysfonctionnement du complexe oxydase. Par exemple, l'étude du canal à proton d'un cas de CGD X^+ a pu être réalisé dans les LB-EBV (Stasia et al. 2002).
3) Tester les approches de thérapie génique (Thrasher et al. 1992; Porter et al. 1993; Maly et al. 1993).
4) Etudier l'interactions entre les composants du complexe oxydase et de nouveaux partenaires (Berthier et al. 2003).

4.2 Les cellules K562

Les cellules K562, caractérisées par une expression endogène de Rac2 et $p22^{phox}$, sont issues des cellules leucémiques myéloides indifférenciées et multipotentes (de Mendez at al. 1995). Ce modèle cellulaire a permis l'étude des interactions entre les facteurs de la NADPH oxidase.

4.3 Les cellules $CD34^+$

La molécule $CD34^+$ est une glycoprotéine exprimée à la surface de 2-4% des cellules médullaires. Cette ligne cellulaire constitue la cible des essais de thérapie cellulaire *ex vivo* (Li et al. 1994) et de thérapie génique (Malech et al. 1997).

4.4 Les cellules PLB-985

Les cellules PLB-985 sont issues d'une lignée cellulaire myélomonoblastique humaine d'une patiente atteinte d'une leucémïe chronique, en phase de rémission (Tucker et al. 1987). Ces cellules ont la capacité de se différencier en monocytes ou granulocytes après addition d'agents de différenciation. Il y a alors induction de l'expression des composants du complexe oxydase avec production d'H_2O_2 (Pedruzzi et al. 2002). Une lignée de cellules X-CGD PLB-985 a été obtenue par recombinaison homologue avec insertion d'une cassette (phosphotransférase hygromycine B) au niveau du exon 3 du gène *CYBB*, cette lignée mime les PMN de CGD X^0, caractérisé par l'absence du cytochrome b_{558} avec une activité oxydase nulle (Zhen et al. 1993). Cette lignée cellulaire est un modèle intéressant pour l'étude du fonctionnement de la NADPH oxydase :

1) Etude des sites fonctionnels de $gp91^{phox}$, la boucle B, la boucle D, l'hélice α (^{484}DESQANHFAVHHDEEKDVITG^{504}), la région C-terminale (^{559}RGVHFIF^{565}), (Zhen et al. 1997 ; Biberstine-Kinkade et al. 1999 ; Li et al. 2005) (Figure 7).
2) Analyse de l'interaction entre $gp91^{phox}$ et $p22^{phox}$ et la maturation du cytochrome b_{558} (Yu et al. 1999 ; DeLeo et al. 2000).
3) Reproduction de mutations géniques humaines (His303Asn/Pro304Arg, Pro 415His, délétion Δ488-497, Asp500Gly) de CGD X^+ pour analyser l'impact de ces mutations sur les mécanismes d'activation et d'assemblage du complexe oxydase (Zhen et al. 1993 ; Yu et al. 1999 ; Bionda et al. 2004 ; Li et al. 2005).
4) Etude des homologues de $gp91^{phox}$ (Geiszt et al. 2003).

4.5 Les cellules fibroblastiques

▸ Les cellules **CHO** (*C*hinese *h*amster *o*vary) sont issues d'une biopsie d'ovaires de hamster. Cette lignée cellulaire a été utilisée pour étudier l'activité canal à protons de $gp91^{phox}$ (Henderson et al. 1997; Henderson et al. 1999; Mankelow et al.2003*b*; Mankelow et al. 2004).

▸ **HEK293**, caractérisée par une expression endogène de 22^{phox} (Maturana et al. 2001; Ambasta et al. 2004), est une cellule embryonnaire hépatique humaine infectée par l'ADN de l'adenovirus type 5. Elle a été utilisée pour étudier le canal à protons (Maturana et al. 2001) et

les homologues de gp91^{phox}, de p47^{phox} (NoxO1 ou p41), et de p67^{phox} (NoxA1 ou p51) (Banfi et al. 2003 ; Banfi et al. 2004 ; Ambasta et al. 2004 ; Cheng et al. 2004).

▸ **COS-7**, est une cellule fibroblastique de rein de singe facilement cultivable et transfectable avec un taux d'expression protéique important. Les cellules COS-7, exprimant Rac1 et p22^{phox}, ont été utilisée pour étudier la maturation du cytochrome b_{558} (Yu et al. 1999 ; DeLeo et al. 2000), le canal à protons (Maturana et al. 2001 ; Murillo et al. 2004), et les homologues de p47^{phox} (NoxO1) et de p67^{phox} (NoxA1) (Takeya et al. 2003).

5. Objectifs du travail

La NADPH oxydase est un complexe multi-protéique dont l'activation dépend de la translocation de ses composants cytosoliques ((p47^{phox}, p67^{phox}, p40^{phox} et Rac) vers la membrane plasmique des phagocytes, pour s'assembler à l'élément redox de cette enzyme, le cytochrome b_{558} lui-même composé de deux sous-unités gp91^{phox} ou Nox2 et p22^{phox}. C'est uniquement dans cette configuration assemblée qu'elle est active et que le transfert électronique au travers du cytochrome b_{558} peut avoir lieu, du NADPH vers l'oxygène moléculaire en passant par le FAD. Ce processus d'activation montre qu'il existe une relation très étroite entre les interactions protéine-protéine et le transfert des électrons pour former les anions superoxide bactéricides.

Un des moyens d'appréhender les mécanismes d'activation du complexe oxydase est l'étude du dysfonctionnement de cette enzyme dans la granulomatose septique chronique, maladie génétique rare. L'étude d'un de ses variants, CGD X^+, est particulièrement intéressante puisqu'il est caractérisé par une expression normale de gp91^{phox} mutée qui n'est cependant pas fonctionnelle. Une relation entre une fonction spécifique de la protéine et le domaine contenant la mutation est alors facile à établir. Cependant les études de structure-activité d'une protéine sont souvent gourmandes en matériel biologique et le nombre de neutrophiles des patients à disposition est le facteur limitant de ce genre d'approche.

Le but principal de ce travail est la compréhension du rôle de certaines régions de gp91^{phox} en utilisant comme méthodologie, la mutagénèse dirigée et la transfection stable dans un modèle cellulaire mimant les neutrophiles d'un patient atteint de CGD-X^0, les cellules X-CGD PLB-985. Ce modèle a été établi par l'équipe de M. Dinauer (Zhen et al. 1993) en utilisant la méthode de recombinaison homologue dans le gène *CYBB* pour réaliser ce knock-out.

1) Le premier travail a consisté à reproduire dans ce modèle un cas de CGD , caractérisé par une double mutation faux-sens, His303Asn/Pro304Arg (Stasia et al. 2002*a*). Cette mutation est localisée non loin du site potentiel de fixation du FAD. Le but a été d'étudier l'impact de la double mutation et de chacune d'entre elles séparément, sur les mécanismes d'activation du complexe oxydase (Chapitre 1).
2) Le second objectif de ce travail a été l'étude du rôle de deux régions de Nox2; la seconde boucle intracytosolique, la boucle D (^{191}TSST**K**TI**RR**S^{200}) et une région de la partie C-terminale cytosolique de Nox2 (^{484}**D**ESQAN**H**FAVHH**D**EEK**D**^{500}). Ces régions chargées et plus particulièrement les acides aminés soulignés, sont très

conservés dans la famille des FNR. La boucle D est localisée dans une région proche du V^{ème} fragment transmembranaire de Nox2 impliqué dans la liaison des hèmes du cytochrome b_{558}. Ceci suggère un rôle potentiel de cette boucle dans l'activation de la NADPH oxydase et/ou dans le maintien de la structure de celle-ci. Cette région n'a pas été étudiée jusqu'alors.

La seconde région à l'étude est une boucle formant une hélice α d'après le modèle 3D de la partie C-terminale de Nox2 proposé par Taylor *et al.* (Taylor et al. 1993). Lorsque l'enzyme est au repos, cette boucle pourrait recouvrir le site de liaison du NADPH localisé dans une sorte de crevasse. Durant l'activation, ce site pourrait se libérer par un mouvement de cette boucle lors de sa liaison avec les facteurs cytosoliques. Des travaux récents ont montré l'importance de cette région dans l'activation de la NADPH oxydase, mais les résultats sont très controversés (Leusen et al, 1994 ; Yu et al. 1999; Tsuchiya et al. 1999). Lors de ce travail une seconde CGD X^+ a été reproduite et étudiée dans ce modèle cellulaire. Il s'agit d'une mutation faux-sens Asp500Gly située dans la boucle en hélice α étudiée (Leusen et al. 1994). Une autre mutation double RR9192EE dans la boucle B préalablement étudiée (Biberstine-Kinkade et al. 1999) a été reconstituée dans le modèle X-CGD PLB-985 afin de valider notre méthodologie (Chapitre 2).

3) Enfin un dernier cas de CGDX^+ dû à une mutation faux-sens Leu505Arg située dans le site potentiel de fixation de l'adénine du NADPH, a été reproduit dans le modèle X-CGD PLB-985. Cette mutation est également située à la fin de l'hélice α étudiée dans le Chapitre 2. Ce résidu est très conservé dans la famille Nox/Duox ce qui suggère l'importance de cet acide aminé et probablement un rôle commun dans cette famille (Chapitre 3).
4) Notre quatrième objectif a été de déterminer le défaut dans la synthèse et /ou la maturation du cytochrome b_{558} dans un cas de CGD X^- dû à une substitution Ser193Phe (Roesler et al. 1999) située dans la boucle D, étudiée dans le Chapitre 2. Deux modèles cellulaires ont été utilisés; les cellules X-CGD PLB-985 et COS-7, ne possédant pas de p22^{phox} pour la première et en possédant pour la seconde. En effet le but était d'étudier l'influence de la présence de p22^{phox} dans la synthèse du cytochrome b_{558} (Chapitre 4).